CORE-LEVEL PHOTOELECTRON SPECTROSCOPY OF SMALL MOLECULES

Contents

CORE-LEVEL PHOTOELECTRON SPECTROSCOPY OF SMALL MOLECULES

Donald William Davis

Department of Chemistry and
Lawrence Berkeley Laboratory
University of California
Berkeley, California 94720

May 1973

ABSTRACT

Relative core-level binding energies and multiplet splittings in binding energies are measured for a number of gases at low pressures and variable temperatures. These measurements are interpreted with CNDO/2 and INDO/2 wavefunctions.

An analysis of the variation in linewidths of the measured photoelectron spectra is given. The Auger effect is shown to account for some, but not all of the variation in the linewidths. An argument is given for the importance of the Franck-Condon principle in core-level photoionization, particularly in highly fluorinated systems.

The Hellman-Feynman theorem is used to derive a quantitative relation between the two most common theoretical interpretations of core-level chemical shifts. The potential-at-a-nucleus approach is used with CNDO/2 wavefunctions to interpret the measurements made here.

INDO/2 wavefunctions are used to interpret the multiplet splittings observed in a number of core-level photoelectron spectra. Koopmans' theorem is shown to be inapplicable to the interpretation of these multiplet splittings.

INTRODUCTION

The subject of this thesis is the core-level photoelectron spectroscopy of gases; this subject will be treated as a subfield of electronic absorption spectroscopy, i.e., the formalism will be the same.

The basic measurement made here is the core-level binding energy. This is the difference between the energy of a state of a molecule with a core vacancy and the ground state energy. During the past ten years, much work has gone into the interpretation of the effect of chemical environment upon core-level binding energies; this thesis will utilize this work and hopefully build upon it a bit. Most of the discussion here of the effect of chemical environment involves the electrostatic potential at a nucleus--perhaps the same might be said about the literature on this subject.

This thesis makes extensive use of CNDO/2 and INDO/2 semi-empirical wavefunctions. These wavefunctions are among the most popular with chemists because they do a fairly good job of mimicking ab initio wavefunctions at low cost. In order to understand this thesis, it is not necessary to know all about semi-empirical wavefunctions; in fact, this thesis was written without such knowledge. Hopefully, however, the reader has some familiarity with the terms of quantum chemistry, such as molecular orbital.

Perhaps the central concept of this thesis is the equivalent cores approximation. This concept equates the state of a molecule with a core-level vacancy to a state which is identical to the ground state of

the molecule, except that the nucleus with the core-level vacancy has its charge increased by one. This concept was introduced into photoelectron spectroscopy by W. Jolly for the purpose of predicting core-level shifts from experimentally determined heats of formation, and has since spread into Auger spectroscopy as well as the prediction of multiplet splitting.

An attempt has been made in this thesis to point out all the assumptions made in the theoretical interpretation of the measurements. Similarly, an attempt has been made to point out systematic errors in the measurements and data analysis. If there is an object to this thesis, it is to determine the usefulness of core-level photoelectron spectroscopy to chemists—not whether it can test the accuracy of wavefunctions, but whether it can tell chemists something about the ground states of molecules.

I. EXPERIMENTAL SECTION

A. General

A simple description of the experiments performed is the following: X-rays of known energy and energy spread strike a gaseous sample; some of the photoelectrons produced enter a magnetic field of known strength. The magnetic field is cylindrically symmetrical and roughly perpendicular to the velocity of the photoelectrons at their point of entrance into the spectrometer. Therefore, the electrons traverse a circular path, at some point of which they may enter an electron detector. Since the magnetic field strength is known and the radius of the path of the photoelectrons is known, the momentum of the photoelectrons may be determined.

A characteristic of the sample called the binding energy is defined by the following energy conservation equation:

$$E_B + K.E. = h\nu \quad . \tag{1}$$

Here, E_B is the binding energy, and K.E. is the kinetic energy; it is determined from the momentum by the usual equations:

$$K.E. = p^2/2m \; ; \quad p^2/2m = mc^2 - m_0c^2 \quad . \tag{2}$$

Here, p is the momentum, c is the speed of light, and m is the mass.

A schematic illustration of the spectrometer is given in Fig. 1. The construction of the spectrometer is discussed in great detail elsewhere.[1] For this study the important points about the spectrometer are the accuracy of relative binding energy measurements, the resolution

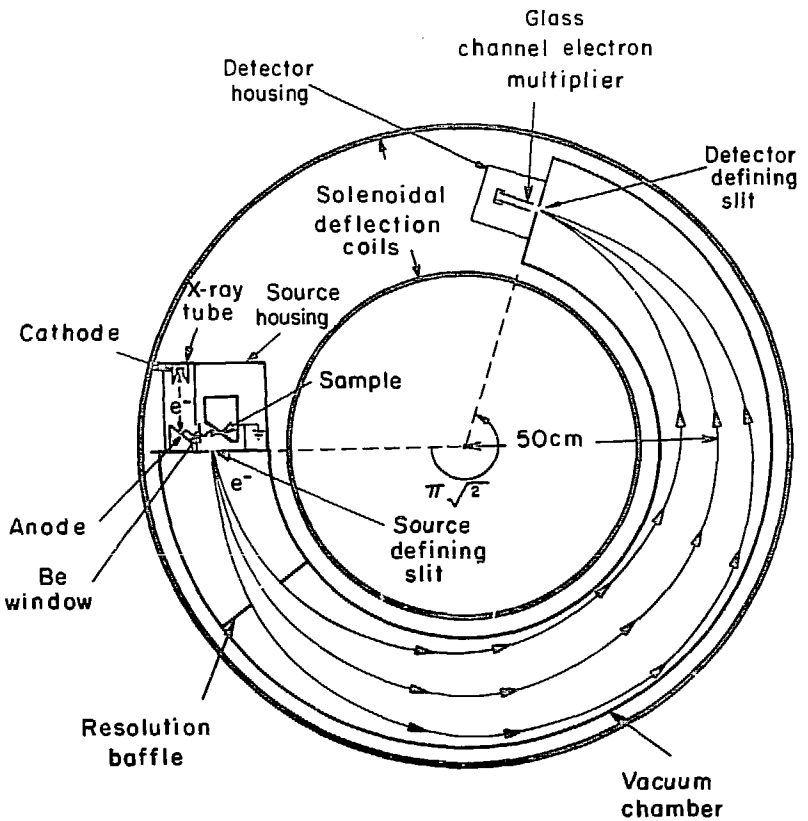

XBL694-2402

Fig. 1. Schematic illustration of the electron spectrometer. The sample indicated is a solid; in order to run gases, a gas cell was substituted for the solid sample holder.

of the spectrometer, and the contribution of the spectrometer to the shape of the observed intensity vs. energy distribution of the photoelectrons.

The spectrometer has been calibrated by Fadley, Geoffroy, Hagstrom, and Hollander;[2] it has been found to measure absolute binding energies within several parts of 10^4; relative binding energies should therefore be measured accurately to within one part in 10^3, or 0.01 eV for a typical range of 10 eV.

The resolution of the spectrometer was set at $\Delta E/E = 0.06\%$ for these experiments--that is, the intensity distribution of a perfectly monochromatic beam of 1 keV photoelectrons focused by this spectrometer would have a width of 0.6 eV FWHM. The lineshape of this peak would be slightly asymmetric, and skewed toward the low kinetic-energy side.

The electron detector is an electron multiplier; the multiplication comes from an electron cascade along a sensitive surface which has a potential of several keV across it. This surface is sensitive to some gases, especially fluorinating agents such as UF_6 and F_2. It does not appear to be affected by most organic compounds or inorganic compounds. The detector is discussed in detail elsewhere.[3]

B. The Gas Sample Cell

In order to contain gaseous samples, a special cell is needed; for gases run at room temperature, one of these had already been constructed;[4] this proved satisfactory. For gases run at higher temperatures, a second cell was constructed. This cell will be discussed later. The room-temperature cell consisted primarily of an

aluminum box with a circular opening to admit x-rays and a slit to allow the passage of photoelectrons and gas into the spectrometer. The slit defines a source of electrons for the spectrometer--for the experiments performed here, the slit was 0.3 mm in width and 1 cm in height.

The pressure inside the aluminum box was in the 10^{-2} Torr range; the pressure was measured by a MacLeod gauge and a thermocouple gauge--the readings agreed within a factor of 2 for most gases. It was not important to know the absolute value of the pressure, but only whether it was constant during an experiment.

The gas flow into the aluminum box was controlled by sensitive double-needle valves (made by Hoke mfg.) or a specially constructed valve consisting of a stainless steel body and a teflon seat (this valve was designed by Gene Miner). The second valve was found to be superior to the first, because it resisted corrosion better and did not leak. For these experiments, the gases were used as received from the manufacturer--any non-negligible impurities were detectable in the spectrometer, but they were rarely present.

In order to study heated samples, another gas cell was designed. The box, slit, and window were copied from the original gas cell. The delicate job of aligning the slit was performed by Salim Banna. Heaters of the type previously used in the spectrometer[4] were constructed by Joe Bryan and attached to the gas cell. These heaters were made of tantalum wire, wound non-inductively, and sandwiched inside slices of boron nitride. To make sure the gas was thoroughly heated before it was exposed to x-rays, it was passed through a 15 cm section of pipe which was heated to the temperature of the box. This idea was taken from

Cornford, et al., who measured the UV photoelectron spectrum of NF_2 above room temperature.[5] We also studied NF_2 at eleveted temperatures, the reason being that it is supplied at high pressures as N_2F_4; although NF_2 is thermodynamically stable at our operating pressures at room temperature, N_2F_4 dissociates very slowly at room temperature, but very rapidly at temperatures around 150° C.

C. The X-Ray Tube

The x-ray tube consists of a cathode (source of electrons), and an anode, which emits x-rays when struck at appropriate energies by the electrons from the cathode. The electrons are accelerated from the cathode to the anode by a voltage of 11 keV applied to the cathode. This voltage was found to be optimal for the production of Mg Kα x-rays.[4] The electrons striking the anode (a piece of magnesium metal) heat it up; this heat is carried away by a water-cooled piece of copper in physical contact with the magnesium. Thus the operation of the x-ray tube requires electrical and fluid vacuum feedthroughs.

In order to run gases for long periods of time (more than one hour), it was found necessary to isolate the vacuum within the x-ray tube from the spectrometer vacuum, because most gases attacked both the anode and cathode. The anode and cooling block assembly were reconstructed so as to allow an o-ring to seal the cooling block to the x-ray tube housing. The anode was screwed directly on to the cooling block rather than squeezed against it indirectly. This design provided more efficient cooling, and it was found by Bernice Mills that the x-ray tube could then be operated at 50% higher power. The other end of the x-ray tube

housing was sealed by simply welding it to the x-ray flange. The beryllium window on the x-ray tube was sealed by placing an o-ring between it and the x-ray tube. The temperature of the x-ray tube housing during operation is slightly over 100° C,[8] so that viton o-rings were necessary. Some cooling of the o-rings was obtained by placing them in contact with water-cooled copper.

The most critical and important aspect of the sealed x-ray tube turned out to be its pumping system. At first a cryopump was used to pump out the x-ray tube, but its pumping speed was too slow; outgassing of the hot cathode and its support dirtied the anode and beryllium window. It was found necessary to pump the x-ray tube by a diffusion pump (this pumping system was constructed by Salim Banna); although the opening from the x-ray tube into the high vacuum was less than two square centimeters, this proved sufficient to keep the anode clean.

D. Systematic Errors

Siegbahn, et al., found that the kinetic energies they measured in the gas phase were a function of the pressure of the gas.[6] They found variations in the measured kinetic energies of up to 1 eV with pressure, and also found that the kinetic energy always decreased with an increase in pressure. They explained this qualitatively as due to positive space or surface charges (e.g. ionized molecules), which would increase in concentration with an increase in pressure. In the Berkeley spectrometer, however, T. D. Thomas found less than a 0.2 eV variation in kinetic energy within the available pressure range.[7] However, in order to minimize this problem as much as possible when measuring chemical shifts, the sample

gas and reference gas were usually run simultaneously. Presumably the space and surface charges affect all the photoelectrons the same way, so relative binding energies are not effected by them.

Another systematic error is the neglect of the transfer of kinetic energy to the molecular ion because of momentum conservation (the momentum of the molecular ion must be equal and opposite to that of the photoelectron). However, for any system heavier than neon, this kinetic energy is negligible.

E. Data Analysis

The raw experimental data consisted of pulses from the electron detector as a function of the current which produced the focusing magnetic field in the spectrometer. The data were taken at discrete current intervals; generally the current was stepped in intervals of 0.0001 or 0.0002 amp. This corresponds to 0.1 to 0.4 eV for the experiments performed here. The data were fitted to Lorentzian peak shapes by a non-linear least-squares fitting program developed by Claudette Lederer.[9] The program works by varying the parameters describing each peak shape, the position of the peak, the area under the peak, and the width of the peak until a "best" fit is obtained by the criterion of a minimum in the value of $\sum_i (E_i - L_i)^2$, where E_i is the i^{th} experimental point and L_i is the i^{th} Lorentzian point. This program fitted the spectra reasonably well, although it is evident that there are systematic errors in using a strictly Lorentzian peak shape--the contribution of the spectrometer to the peak shape is not Lorentzian, and there are also some discrete and

continuous energy-loss satellites on the low kinetic energy side of the peaks, which of course could not be accounted for by the Lorentzian shape.

A measure of the quality of a fit is the weighted variance:

$$W.V. = (1/N) \sum_i (E_i - L_i)^2/E_i \quad . \tag{3}$$

Here, N is the total number of points fitted. Now the experimental uncertainty in E_i is about $(E_i)^{.5}$, so a good fit should give L_i to within $(E_i)^{.5}$ of E_i. Therefore the weighted variance for a good fit becomes $(1/N) \sum_i ((E_i)^{.5})^2/E_i$, or about 1. For most of the spectra fitted, the weighted variance was between 3 and 10. Such fits gave peak positions to within ±0.03 eV, and the width (at half of the maximum) to within ±0.1 eV. Examples of spectra and their fitted peaks are given in Figs. 2a and 2b.

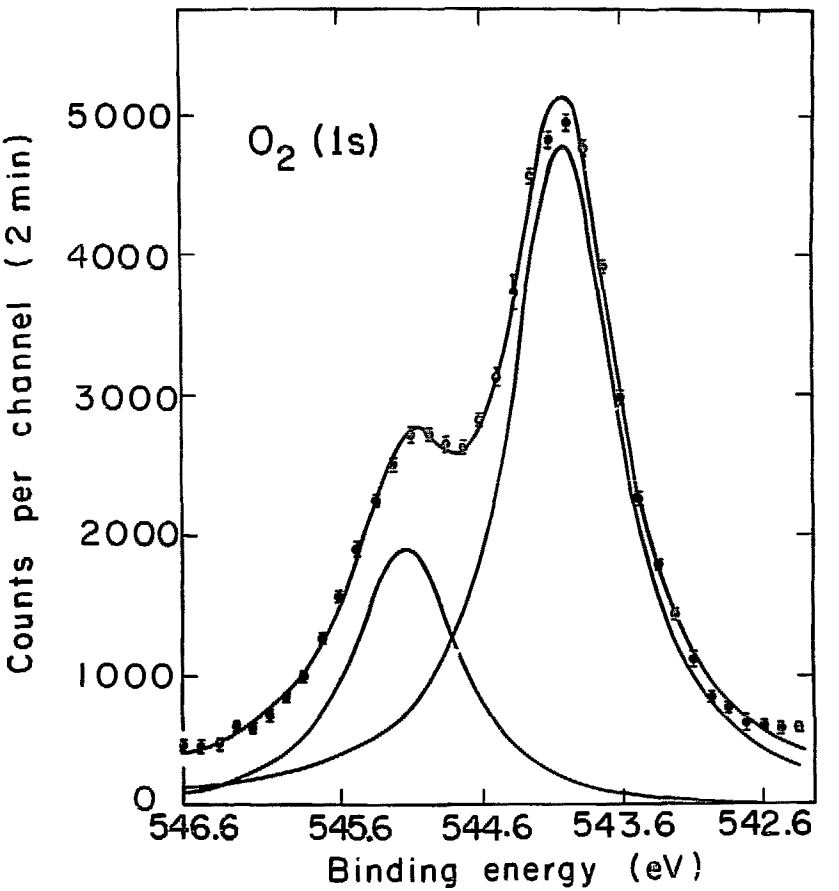

XBL704-2735

Fig. 2a. Spectrum of the 1s photoelectrons of molecular oxygen, a paramagnetic molecule. The experimental data are indicated by points. The fitted Lorentzian functions are indicated by solid lines.

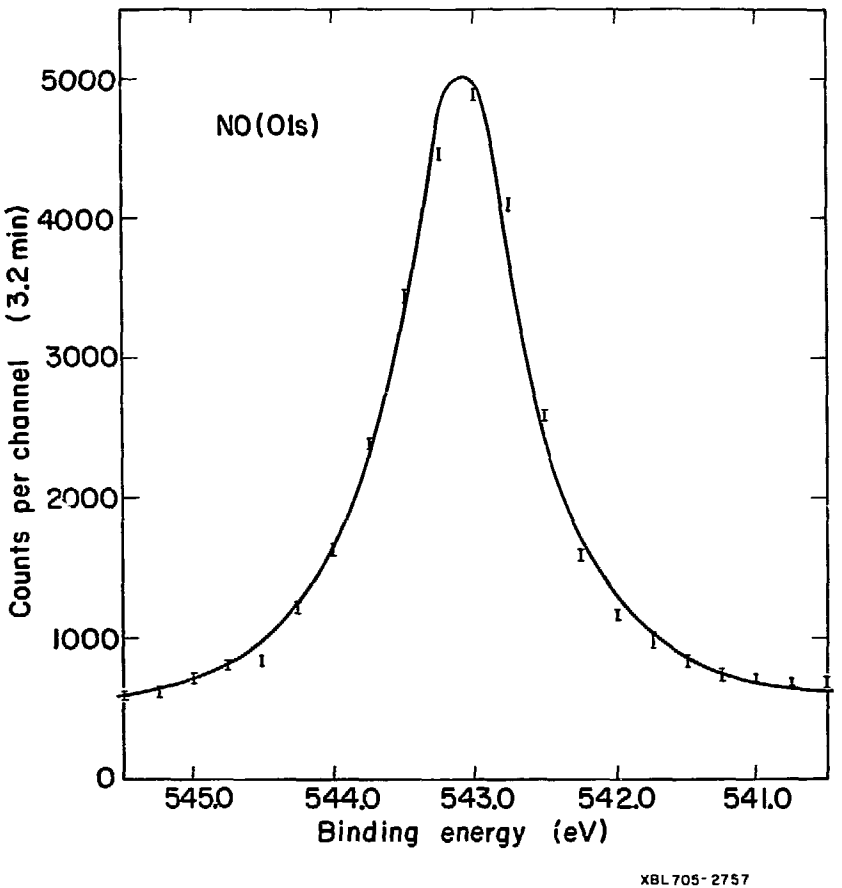

Fig. 2b. Spectrum of the oxygen 1s photoelectrons of the paramagnetic molecule, nitric oxide. The fitted function consists of one peak, instead of two, and therefore it fits the data poorly.

SECTION II. DISCUSSION OF CORE BINDING ENERGIES

The basic experiment performed in this work may be described formally as follows: a molecule in its ground state, with a kinetic energy equal to kT (T $\sim$ 300° C) exists in a radiation field; at some time t_0, a photon with an energy of about 1 keV enters the vicinity of the molecule. There is a probability that the molecule absorbs the photon--if a core electron is emitted after absorption of the photon, the resulting ion may decay via radiative or radiationless transitions (emission of a photon or emission of electrons). The ion may then dissociate.

It is obvious that to describe fully and quantitatively the behavior of the system would be very difficult. Fortunately, for the systems studied here (low atomic number), the interaction of the system with radiation fields can be almost totally neglected. First of all, quantum-electrodynamical effects will be below the limits of experimental error, and second, non-radiative transitions in the ion are much more likely than radiative transitions. In fact, only the lineshape of the exciting radiation and its energy are important here. The energy of the radiation is used to define a characteristic of the molecule called the binding energy:

$$h\nu = \text{B.E.} + \text{K.E.} \quad . \tag{1}$$

Here, $h\nu$ is the energy of the exciting radiation, K.E. is the experimentally measured kinetic energy of the photoelectron, and B.E. is the binding energy. The binding energy depends on the ground state of the molecule and the state of the ion formed immediately after emission of the

photoelectron. The non-radiative transitions are important because they affect the measured linewidth of the photoelectron; later, an attempt will be made to assess the magnitude of the effect for the systems studied here.

The core photoelectrons measured in this work have velocities of about 10^9 cm per sec; within 10^{-15} sec, the photoelectron and ion are essentially separated. While the photoelectron is within the vicinity, i.e., within $\sim$ 100 Å of the remainder of the molecule, this remainder, or ion, may be described as a "quasi-bound" state; that is, a state where all the electrons are in "bound" states, but a vacancy exists in an inner shell. This "quasi-bound" state is not a stationary state, because one of the electrons in higher shells may fill the inner shell vacancy. This filling is accompanied by the ejection of another electron (again, from a higher shell) from the molecular ion. This, of course, is the non-radiative transition. Its rate determines the lifetime of the "quasi-bound" state; this lifetime gives an uncertainty to the kinetic energy of the photoelectron through the uncertainty principle. The non-radiative transition rates seem to be accurately calculable within the formalism of one-electron wavefunctions and time-dependent perturbation theory;[10] the probability for such transitions is proportional to the square of the matrix element of $1/r_{12}$ between the "quasi-bound" state and the de-excited, continuum state.[10] (Although $1/r_{12}$ does not depend on time, it may be given a time dependence by multiplying it by a factor of $e^{i\omega t}$ and then letting ω go to zero after the calculation of the probability for the transition.[11] $1/r_{12}$ is part of the Hamiltonian of the one-electron wavefunctions, but there are still matrix elements of $1/r_{12}$ between certain

of these functions. The true wavefunction of the ion is a superposition of the "quasi-bound" wavefunction and continuum wavefunctions.)

It is usually assumed in this field that the "quasi-bound" state of the ion is the important one for the determination of the binding energy of the core photoelectron. Implicit in this assumption is the complete relaxation of the valence electrons into their "quasi-bound" orbitals and transfer of this relaxation energy to the photoelectron while it is in the vicinity of the ion. This assumption may not hold for very large molecules or for very fast photoelectrons, but there are as yet no indications that it breaks down.

The final state of the whole molecule (ion + photoelectron) will be assumed here to have a wavefunction of the form

$$\Psi = \psi_{ion}\, \xi \quad ,$$

where ξ is the wavefunction of the photoelectron and ψ_{ion} is the "quasi-bound" wavefunction for the remaining electrons and nuclei. The interaction of the photoelectron and the ion will be neglected. In this approximation $E_{final} = E_{ion} + K.E.$ Let E_0 represent the ground-state energy of the molecule. Since $E_{final} = E_0 + h\nu$, $K.E. = E_0 + h\nu - E_{ion}$. Now since $E_B = h\nu - K.E.$, by Eq. (1), it follows that $E_B = E_{ion} - E_0$.

The Born-Oppenheimer approximation will be assumed here[12] to apply to the ground state and ion, so that their wavefunctions take the form

$$\psi = \psi_{elec}\, \psi_{vib}\, \psi_{rot}\, \psi_{trans} \quad .$$

The energy corresponding to ψ_j is

$$E_j = E_{elec}(e_j, R_{0j}) + E_{vib}(v_j, \nu_j) + E_{rot} + E_{trans} \quad ,$$

where the lower case letters in parentheses represent the various sets of quantum numbers which describe the state j. R_{0j} represents the set of equilibrium internuclear distances, and ν_j represents the set of frequencies describing nuclear motion. Rotational and translational motion are not described in more detail because they are not expected to contribute to the binding energies of core electrons beyond the limits of experimental error. Therefore the expression for the binding energy becomes

$$E_B = E_{ion} - E_0 = \Delta E_{elec}(e_j, R_{0j}) + \Delta E_{vib}(v_j, \nu_j) \quad . \qquad (4)$$

A further approximation is usually made in this field, which considerably simplifies Eq. (4)--it is assumed that the potential curves of the ground state and the "quasi-bound" state are <u>identical</u>, except for a relative displacement along the energy axis. This is equivalent to $\Delta E_{vib} = 0$, as well as $\Delta R_{0j} = 0$. Using this approximation, Eq. (4) becomes

$$E_B = \Delta E_{elec}(e_j, R_{00}) \quad . \qquad (5)$$

This equation will be used here for interpreting binding energies, although cases in which this approximation may break down will be pointed out.

The error in Eq. (5) may be easily estimated as follows: rearrange Eq. (4) to read

$$E_B = E^{ion}_{elec}(e_i, R_{OO}) - E^{O}_{elec}(e_O, R_{CO}) + [E^{ion}_{elec}(R^{ion}_{Oi}) - E^{ion}_{elec}(R_{OO})]$$

$$+ [E^{ion}_{vib}(v_j, \nu_j) - E^{O}_{vib}(v_O, \nu_O)] \quad .$$

The terms in brackets are the errors in Eq. (5); the first term in brackets is always less than zero, and for ΔR less than 0.1 Å, which seems to be the case here, its magnitude is about 0 to 0.3 eV. The second term may be greater or less than zero. Its magnitude will also be of the order of tenths of an eV, unless the ion is highly excited vibrationally. In the next section, this possibility will be examined.

SECTION III. LINEWIDTHS

A. Introduction

The experimental linewidths of core photoelectrons were measured along with their relative binding energies. The linewidths varied with chemical structure, so an attempt was made to explain this variation. Table I indicates the range of linewidths. Furthermore, these variations may affect the interpretation of core-level chemical shifts. In particular, if a line is broadened because of Franck-Condon factors, the experimentally measured binding energy may correspond to a final state which is highly excited vibrationally, and which therefore cannot be treated by Eq. (5).

Now the Franck-Condon principle is one possible cause of the observed variations in linewidth--in valence electron transitions, the Franck-Condon envelope may extend over more than one eV.[13] But the Franck-Condon principle applies to final states which are dissociated as well as to those which are bound; in fact, electronic transitions to dissociated final states may be broadened as much as those to bound final states.[14]

Another possible cause of the observed linewidths is the lifetime of the "quasibound" state. Recently, Shaw and Thomas[15] and Friedman, Hudis, and Perlman[16] have independently ascribed the observed variations in core-level linewidths to such lifetimes. Shaw and Thomas found a correlation of the observed linewidths with the experimental binding energies--as binding energies decreased, the linewidths increased. The explanation given for this is that the binding energies decrease with an increase in electron density at the atom to be ionized (Coulomb's

Table I. Linewidths (eV)

Molecule and core level		w_{spec}	w_{Auger}	$(w_{spec}^2 + (w_{Auger} + w_{rad})^2)^{1/2}$	w_{exp}
CF_4	C 1s	0.57	0.07(7)	0.81(12)	0.88(7)
$C^*H_3CF_3$	C 1s	0.57	0.10(10)	0.84(15)	1.17(7)
CO_2	C 1s	0.57	0.07(7)	0.81(15)	1.02(10)
CO	C 1s	0.57	0.07(7)	0.81(12)	0.94(7)
CO	O 1s	0.43	0.20(20)	0.85(25)	0.78(10)
CO_2	O 1s	0.43	0.21(21)	0.86(26)	0.96(10)
NNO	O 1s	0.43	0.21(21)	0.86(26)	0.91(10)
N^*NO	N 1s	0.51	0.14(14)	0.85(19)	0.91(10)
NN^*O	N 1s	0.51	0.12(12)	0.82(17)	0.87(10)
N_2	N 1s	0.51	0.13(13)	0.80(18)	0.83(10)
HF	F 1s	0.34	0.25(25)	0.88(30)	0.94(7)
Ne	Ne 1s	0.23	0.26(26)	0.79(31)	0.73(5)
HF	F 1s	0.34	0.25(25)	0.88(30)	0.94(7)
CH_3CH_2F	F 1s	0.34	0.25(25)	0.88(30)	1.22(7)
CH_2F_2	F 1s	0.34	0.25(25)	0.88(30)	1.35(10)
CHF_3	F 1s	0.34	0.25(25)	0.88(30)	1.46(7)
CF_4	F 1s	0.34	0.25(25)	0.88(30)	1.58(7)

In this table, w_{rad} is assumed to be 0.5 eV; w_{spec} is assumed to have an error of 0.05 eV. The error in the third column is the sum of the errors in w_{spec} and w_{Auger}. The error in w_{Auger} is equal to the value of w_{Auger}. w_{exp} is obtained from least-squares fits of a Lorentzian line shape to the experimental data.

Law), while the Auger transition rates increase; this decreases the lifetime of the final state and increases the uncertainty in the kinetic energy and binding energy.

This line of reasoning will be pursued here, and it will be shown that it explains much of the variation in linewidth, but not all of it--in particular, it cannot explain the variation in the fluorine 1s linewidths. An argument will then be given for the relevance of the Franck-Condon principle to F 1s linewidths.

B. Lifetime of the "Quasibound" State

The matrix element which describes Auger transitions is the following:

$$\iint \psi_{1s}(1)\, \xi(s)\, 1/r_{12}\, \psi_i(1)\, \psi_j(2)\, d\tau_1\, d\tau_2 \quad .$$

Electron number one falls from molecular orbital i in the "quasibound" state into the vacant 1s orbital, and the second electron carries energy away by making a transition from molecular orbital j into a continuum orbital.[10] It is expected that the major part of this matrix element is the following one-center integral:

$$c_{j\ell}\, c_{ik} \iint \psi_{1s}(1)\, \xi(2)\, 1/r_{12}\, \phi_k(1)\, \phi_\ell(2)\, d\tau_1\, d\tau_2 \quad .$$

Here $c_{ik}\, \phi_k$ is the part of ψ_i centered on the ionized atom, and $c_{j\ell}\, \phi_\ell$ is the corresponding part of ψ_j. The actual integral will be called A(i,j); the <u>total</u> Auger transition rate is then roughly proportional to the term

$$\sum_{i,j} (c_{ik}\, c_{j\ell})^2\, A^2(i,j) \quad .$$

A(i,j) does not depend very strongly on its constituent atomic orbitals,[10] and the sum over the coefficients should be roughly proportional to the square of the density of the valence electrons at the ionized atom in the "quasi-bound" state. Therefore, the total Auger transition rate in a molecule should be roughly proportional to the square of the valence electronic population at the ionized atom.

There are available in the literature calculated Auger transition rates for first row atoms (e.g. McGuire[10] and Walters and Bhalla[10]), but not for molecules. However, it seems reasonable that the major difference between atomic and molecular Auger rates should be the differences in the valence electronic populations at the ionized atoms. This population does not change upon core ionization in atoms, but it generally increases by about 0.5 to 1 electron in molecules (according to CNDO/2 estimates). An estimate of this population will be obtained with the equivalent cores approximation and CNDO/2 wavefunctions,† and together with the theoretical results for atoms, it will be used to estimate the contribution of Auger transitions to experimentally observed linewidths.

McGuire's calculations give the following for the energy uncertainty of 1s "quasi-bound" states in atoms: C, 0.06 eV, N, 0.09 eV, O, 0.15 eV, F, 0.22 eV, Ne, 0.26 eV. CNDO/2 wavefunctions indicate that the valence electron density at carbon in the equivalent-cores ion varies from 4 to about 5.2. Thus, the energy uncertainty should vary from about 0.06 eV to about 0.2 eV (a factor of two allowance is made for the crude nature of

†CNDO/2 wavefunctions are widely-used semi-empirical wavefunctions; their calculation is discussed in detail in Ref. 24.

this approach). The analogous results for nitrogen are 0.09 to 0.25 eV; oxygen, 0.2 - 0.3 eV; no CNDO/2 results are available for the core-ionized state of fluorine, but because fluorine is always negatively charged in molecules, it is expected that the variation in its Auger lifetime should be quite small. Assuming a valence population of about 8 on the ionized atom, the energy uncertainty becomes 0.26 eV.

In order to test these numbers with experimental measurements, one must know the relationship between the uncertainty in the energy and the experimental linewidth. This is not a direct relationship, because the experimental line shape is affected by the spectrometer resolution and the shape of the exciting radiation. In fact, the necessary relationship is not exactly known—all that exists is a rough rule of thumb. What is definitely known is that the exciting radiation has a Lorentzian lineshape and a FWHM of 0.4 to 0.5 eV.[6] (Although the radiation hits the sample as a spin-orbit doublet, the fitting program corrects for this.) The lifetime of the quasi-bound final state also contributes a Lorentzian line shape; these two contributions are convoluted to give another Lorentzian line shape whose FWHM is the sum[43] of the widths of the lifetime and the radiation:

$$\text{width}_{\text{convolution}} = \text{width}_{\text{Auger}} + \text{width}_{\text{radiation}} \quad .$$

This relation is peculiar to Lorentzian line shapes; for Gaussian line shapes, the width of the convolution is the square root of the sum of the squares of the contributing widths. What is unknown is the relation between the experimentally observed width ($\text{width}_{\text{exp}}$), the spectrometer

resolution ($width_{spec}$), and the width of the convolution. The rule of thumb which seems to work is the following:

$$width_{exp} = ((width_{exp})^2 + (width_{convolution})^2)^{1/2} \quad . \qquad (6)$$

This rule could be made slightly more accurate by varying the exponents, but it is qualitatively correct. Table I gives a comparison of the calculated width and the observed width. It is evident that the Auger effect accounts for some of the variation in linewidth, but it cannot explain the variation in the carbon 1s linewidth or that of the F 1s linewidth. Equation (6) may be partly to blame for the small range of the predicted linewidths, but even if the observed linewidths increased linearly with the width of the convolution, the Auger effect alone could not account for the range in either the carbon linewidth or the fluorine linewidth.

C. The Franck-Condon Principle

When a molecular system absorbs energy and makes a transition corresponding to the excitation of an electron, some of the energy may be absorbed by the relative motion of the nuclei. Because the final state has a number of vibrational levels, several peaks or bands of varying intensity may be observed in each electronic transition. If the nuclei are dissociated, the vibrational excitation causes the spectrum to be diffusely broadened. Vibrational excitation is observed in optical absorption spectroscopy and UV photoelectron spectroscopy. This effect can be explained by the well-known Franck-Condon principle;[13] this

principle states that the probability for excitation to a given vibrational level in the final state is approximately proportional to the square of the overlap integral between the ground state and final state vibrational wavefunctions. This effect has so far not been directly observed in x-ray photoelectron spectroscopy because the instrumental resolution is not high enough. However, vibrational excitation may contribute to the width of the observed peak.

To check on the possibility of vibrational broadening in core-level spectroscopy, the probabilities of excitation in various vibrational levels upon core ionization were calculated for the diatomic molecules HF, CO, and N_2. These probabilities (commonly called Franck-Condon factors) were calculated within the harmonic oscillator approximation, using a method due to Manneback.[38] The final state was assumed to be an equivalent-cores ion, and published bond lengths and frequencies were used. In the harmonic oscillator approximation, the Franck-Condon factors depend on four parameters--the change in equilibrium internuclear distance for the transition (ΔR_{0j}), the reduced mass μ ($m_1 m_2/(m_1 + m_2)$, and the two vibrational frequencies ν_0 and ν_i. To check on these calculations, Franck-Condon factors were also calculated for the ionization of the least-bound electron in NO, for which experimental Franck-Condon factors are available.[13] The results are shown in Table II.

The assumption of harmonic oscillator wavefunctions is obviously not very good, but it does give some indication of the importance of Franck-Condon factors for core-level ionization in these molecules. No attempt was made to calculate Franck-Condon factors for polyatomic molecules because of the difficulty of the calculation and the lack of parameters, especially R_{0j}.

Table II. Franck-Condon Intensity Ratios

Transition	0-1/0-0	0-2/0-0	0-3/0-0
NO to NO^+ (expt)	1.5	1.4	1.0
NO to NO^+ (theory)	1.3	0.4	0.06
HF to NeH^+ (theory)	0.28	0.002	0.0007
CO to NO^+ (theory)	0.74	0.13	0.013
CO to CF^+ (theory)	0.01	0.0004	0.00001
N_2 to NO^+ (theory)	0.14	0.004	0.00003

The C 1s line in CO should be broadened the most, of the cases tested. The observed width for CO exceeds the calculated width by 0.13 eV, which is somewhat more than for the other cases tested in Table II, and it is also slightly more than for the C 1s line in CF_4, which on the basis of lifetimes only is calculated to have the same linewidth.

When polyatomic molecules are considered, the difference between experiment and theory becomes greater. The observed widths of the C 1s line in CO_2 and the "CH_3" C 1s line in CF_3CH_3 are considerably broader than the calculated values in Table I; the F 1s lines show an even greater discrepancy between theory and experiment in Table I. What is striking about the F 1s widths is the large increase in observed width with successive fluorination at the carbon atom, whereas the calculated widths do not change with fluorination. It was assumed in the calculations that the net electronic population at the ionized fluorine atom would remain constant with fluorination (although estimates of these populations are not available) because both CNDO/2 and ab initio[41] ground state populations at fluorine remain constant with fluorination.

In order to get an indication of the effect of vibrational excitation on core-level linewidths in polyatomic molecules, a study was made of the dependence of diatomic Franck-Condon factors upon the necessary parameters. The Franck-Condon factors calculated with parameters corresponding to polyatomic molecules should give a rough idea of the importance of vibrational excitation for core-level transitions in polyatomic molecules. For this study, ΔR_{0j} was varied between 0 and 0.2 Å, μ was varied between 1 and 10, and the frequencies were varied between 0.1 eV and 0.4 eV. This study indicated that the

Franck-Condon envelope should broaden with increases in these parameters, especially the change in internuclear distance upon ionization. Traditionally, the ionization of "non-bonding" electrons such as core-level electrons causes little or no change in R_{0j}, and hence causes little vibrational excitation.[13] However, even in diatomic molecules the change in R_{0j} upon core ionization can be comparable to that resulting from the ionization of bonding or anti-bonding valence electrons. For example, ΔR_{0j} for the transition CO to NO^+ is about 0.06 Å, and for HF to NeH^+ it is 0.07 Å, while for the ionization of the least-bound (anti-bonding) electron in NO, it is about 0.08 Å.[39] It is expected that ΔR_{0j} can be larger for polyatomic molecules, because R_{0j} is larger, and also, core ionization affects the valence levels to a greater extent in polyatomic molecules than in diatomic molecules.[26] As previously mentioned, values of R_{0j} are unavailable for many polyatomic systems, especially the ions. However, a few calculated values have been found for the equivalent-cores ions, and they indicate that ΔR_{0j} can be as large as 0.2 Å for a core-level transition[47] (in particular, for the transition NOF to NF_2^+, ΔR_{0j}(N-O) is 0.24 Å and ΔR_{0j}(N-F) is -0.15 Å[48]). Such large values of ΔR_{0j} will probably result in considerable vibrational excitation in the ion. For ΔR_{0j} = 0.1 Å, μ = 8, and ν_i and ν_f = 0.1 eV, the ratios of calculated diatomic Franck-Condon factors were as follows: 0-1/0-0 = 1.71, 0-2/0-0 = 0.57, and 0-3/0-0 = 0.08. Thus, if the experimental Franck-Condon factors for such a transition exceed the calculated values as for the transition NO to NO^+ in Table II, the Franck-Condon envelope would have a FWHM of at least 0.5 eV. This is sufficient to explain the

variation in the C 1s linewidths, while a somewhat broader envelope would be required to explain the F 1s linewidths. However, such a possibility is not excluded by these crude calculations.

In order to gain more insight into the processes which may be broadening the F 1s spectra, published[41] UV photoelectron spectra of the fluoromethanes were examined. Almost all of the peaks were broadened, but many of the peaks had no visible Franck-Condon envelope. The explanation given for this broadening is dissociative ionization; i.e., the broadening is still due to vibrational excitation, but the overlap occurs between the bound vibrational wavefunction in the ground state and continuum vibrational wavefunctions in the ion. This explanation is supported by the fact that the mass spectral peaks corresponding to many of the ions of the fluoromethanes have not been observed.[41] However, there are no "non-bonding" or "lone-pair" valence electrons in the fluoromethanes, so perhaps these spectra are unrelated to the core-level spectra. With this in mind, the UV photoelectron spectrum of the Cl "lone-pair" valence electrons in CF_3Cl was measured.[42] The Cl "lone-pair" valence electrons were expected to behave similarly upon ionization to the F and Cl core levels, because they are essentially localized on one atom. However, the vacancy left after ionization of these electrons is not completely localized at the Cl atom; CNDO/2 wavefunctions indicate that 50% of the vacancy lies on other atoms. The spectrum of the Cl "lone-pair" valence electron consisted of a single symmetrical peak with a FWHM of about 0.6 eV, but no Franck-Condon envelope was visible. This peak was about 0.5 eV broader than the corresponding peak in CH_3Cl. It

is similar in appearance to the smoothly broadened peaks in the UV spectra of the fluoromethanes; for this reason, it seems likely that the peak is broadened because of dissociation in the final state. In our opinion, this is indirect evidence for dissociative broadening in core levels. However, this question cannot be settled until more information is available. Theoretical calculations of the relevant potential surfaces would be helpful.

If dissociation occurs upon core ionization, then vibrational excitation must also occur. In other words, the maximum of the experimental peak must correspond to a state of the ion which lies above the lowest point(s) in its potential curve (even if there is no minimum in the potential curve). Figure 3 illustrates this point. Thus, the vibrational energy of the final state should be taken into account when calculating chemical shifts. No attempt was made to calculate this vibrational energy, but theoretical calculations which neglect it[41] predict the experimental shifts well. So perhaps the excess vibrational energy is unimportant or cancels out when taking relative binding energies.

D. Conclusions

Variations in the lifetime of the "quasi-bound" final state explain some, but not all of the variations in core-level linewidths. Vibrational excitation in the final state seems to be the most likely cause of broadening in core levels. It may contribute to binding energies to the extent of several tenths of an eV. The F 1s levels are probably broadened because of dissociation in the "quasi-bound" final state.

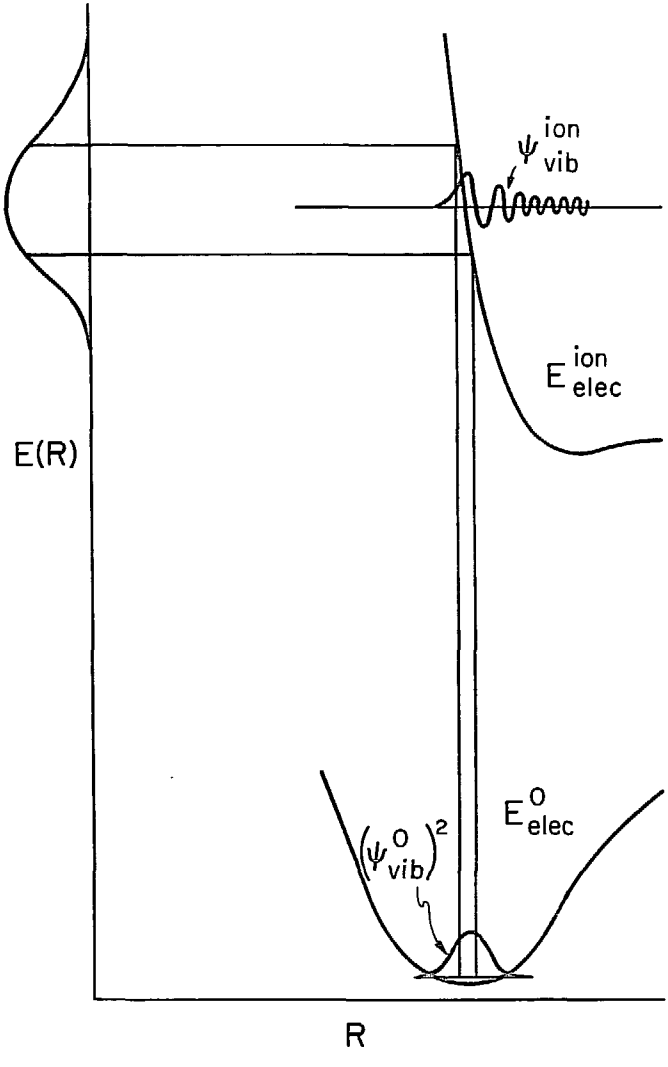

XBL 735-2837

Fig. 3. This figure is adapted from Ref. 14, p. 392. It indicates the broadening which can occur because of transitions to a dissociated state. The spectrum is essentially a reflection of $(\psi^0_{vib})^2$ against the repulsive potential curve in the final state.

SECTION IV. CHEMICAL SHIFTS

A. Introduction

Chemical shifts in core-level binding energies are of considerable interest to chemists because they can give information about electronic structure. One of the most common interpretations of chemical shifts involves the use of Koopmans' Theorem.[49] In this interpretation, the core-level binding energy equals the negative of the core-level eigenvalue determined from a self-consistent field wavefunction for the ground state of the molecule. This approach is potentially very useful to chemists because it interprets binding energy shifts entirely in terms of ground state properties. For example, the 1s binding energies obtained using Koopmans' Theorem have been found to co relate linearly with atomic charges.[50] However, such binding energies do not agree with experimentally observed binding energies. They always exceed the observed binding energies, usually by about 5%; such an excess is larger than the total range of chemical shifts for the element, so one must be very careful when applying Koopmans' Theorem to chemical shifts. The difference between the experimentally observed binding energy and that obtained from Koopmans' Theorem is called the relaxation energy. One of the main objectives of this section is to analyze the variation in relaxation energy with chemical environment in order to determine when it can be safely neglected.

CNDO/2 wavefunctions will be used here to obtain relaxation energies and interpret chemical shifts; this is probably the weak point of this section. However, the CNDO/2 theoretical chemical shifts compare well with experiment for a large variety of molecules, and their calculation involves little expense.

B. General Discussion

The expression developed for the binding energy was Eq. (5):

$$E_B = E^{ion}_{elec}\ (e_i,\ R_{00}) - E^{0}_{elec}\ (e_0,\ R_{00}) \quad . \tag{5}$$

Here, E^{ion}_{elec} is the "quasi-energy" of a "quasi-bound" state--a state in which the variational principle is applied to only some of the parameters in the electronic wavefunction in order to preserve an inner shell vacancy. It should be remembered that Eq. (5) can be in error by several tenths of an eV, as discussed in Secs. II and III.

Chemical shifts are calculated simply by taking changes in E_B. In this thesis, $E^{ion}_{elec}\ (R_{00})$ will be approximated by the energy of the equivalent-cores ion. It has been shown empirically by Jolly and co-workers[17] that such an approximation is usually very good; furthermore, theoretical support for the equivalent-cores (or thermochemical) approximation has been given by Shirley.[18] The error in the equivalent-cores approximation is unknown, although Refs. 17 and 18 indicate that when taking chemical shifts it is no more than a few tenths of an eV.

Using the equivalent-cores approximation, Eq. (5) becomes

$$E_B = E_{elec}\ (R_{00},\ Z^0_a + 1) - E_{elec}\ (R_{00},\ Z^0_a) \quad , \tag{7}$$

where R_{00} represents the set of equilibrium internuclear distances in the ground state, and Z^0_a is the charge on nucleus a in the ground state. Equation (7) may be reduced to a simpler expression via the Hellman-Feynman Theorem. This theorem states that

$$\frac{\partial E}{\partial \lambda} = \langle \psi(\lambda) | \frac{\partial \mathcal{H}}{\partial \lambda} | \psi(\lambda) \rangle \quad , \tag{8}$$

where λ is some variable parameter in the Hamiltonian.[19] λ may be one of the internuclear distances, one of the nuclear charges, etc. Here we will take λ to be the nuclear charge on atom a, Z_a. In this case,

$$\frac{\partial \mathcal{H}}{\partial Z_a} = \sum_{j \neq a} \frac{e^2 Z_j}{R_{ja}} - \sum_i \frac{e^2}{r_{ia}} \quad ,$$

where r_{ia} is the distance between nucleus a and electron i, and R_{ja} is the distance between nucleus j and nucleus a. This expression was obtained simply by differentiating with respect to Z_a the usual non-relativistic Hamiltonian for a molecule.

Now $\langle \left| \frac{\partial \mathcal{H}}{\partial Z_a} \right| \rangle$ is the negative of the potential energy of an electron at nucleus a, and will be denoted $-V_a(Z_a)$. It is obviously a function of the value of Z_a. Next, Eq. (8) may be integrated from Z_a^0 to $Z_a^0 + 1$ to give E_B in terms of $V_a(Z_a)$:

$$\int_{Z_a^0}^{Z_a^0 + 1} \frac{\partial E}{\partial Z_a} dZ_a = E(Z_a^0 + 1) - E(Z_a^0) = -\int_{Z_a^0}^{Z^0 + 1} V_a(Z_a)\, dZ_a \quad . \tag{9}$$

Equation (9) is the quantitative relation between the thermochemical model of chemical shifts and any potential-at-a-nucleus models of chemical shifts. This integration of the Hellman-Feynman Theorem has been done previously[20] but so far it has not been applied to physical problems. Obviously, the integral must be simplified to give useful results; in fact, this will be done in such a way that semi-empirical wavefunctions

can be used to estimate chemical shifts. This simplification is guided by the results obtained by other workers.[21] The semi-empirical wave-functions do not have to satisfy the relation

$$\frac{d}{dZ}\langle\psi|\mathcal{H}|\psi\rangle = \langle\psi|\partial\mathcal{H}/\partial Z|\psi\rangle \quad ,$$

but they should give realistic values of V_a.

First, Eq. (9) will be rewritten as

$$-\int_{Z^0}^{Z^0+1} V_a(Z_a)\,dZ_a = -V_a(Z_a^0) - \int_{Z^0}^{Z^0+1} (V_a(Z_a) - V_a(Z_a^0))\,dZ_a \quad .$$

The second term on the right side of the equation will be called the relaxation energy, R. It represents the change in E_B due to the rearrangement of the valence and un-ionized core electrons during core photoemission. When R is the same for two molecules,

$$\Delta E_B = -\Delta V(Z_a^0) \quad .$$

This is an important result--in this case, ΔE_B can be interpreted in terms of ground state properties, and the thermochemical model becomes equivalent to the ground state potential model of chemical shifts. For this reason, an attempt will be made to estimate R (and $V_a(Z^0)$) for various molecules, to see if there are trends in the value of R which enable us to use the ground state model of chemical shifts. This model has already been developed by other workers through the use of Koopmans' Theorem.[21] However, there has not yet been a systematic study of relaxation energies.

In order to make estimates of R, $V_a(Z)$ will be assumed to be a linear function of Z between the values of Z^0 and $Z^0 + 1$; R then turns out to be $1/2(V_a(Z^0 + 1) - V_a(Z^0))$. Heden and Johansson[22] have derived a similar result for Hartree-Fock wavefunctions; the choice of a linear V_a was motivated by their result. The error in the linear approximation may be seen in the graph of V_a versus Z_a (4); the error is the area between the curved line and the straight line, both of which connect $V_a(Z^0)$ and $V_a(Z^0 + 1)$. It is only about 1 eV, with a possible variation from molecule to molecule of only several tenths of an eV. The relaxation energy is the area inside the triangle with the dashed sides. The potentials were calculated with CNDO/2 wavefunctions.

A further assumption will be made in evaluating R and V_a—the contributions of the inner electrons on atom a to R and V_a will be assumed to be the same regardless of chemical environment. Schwartz[21] has investigated this assumption for V_a and found it to be a very good one. With this assumption, it is now possible to evaluate R and V with valence electron wavefunctions and use them to interpret chemical shifts.

C. CNDO/2 Potential Models

The CNDO/2 wavefunction is a molecular orbital wavefunction; that is, the total wavefunction is an anti-symmetrized product of one-electron wavefunctions called molecular orbitals. The total wavefunction could be a linear combination of such anti-symmetrized products, in which case it would be called a configuration-interaction wavefunction; however, for simplicity, it is limited to one configuration.

The molecular orbitals are linear combinations of atomic orbitals centered at the various nuclei:

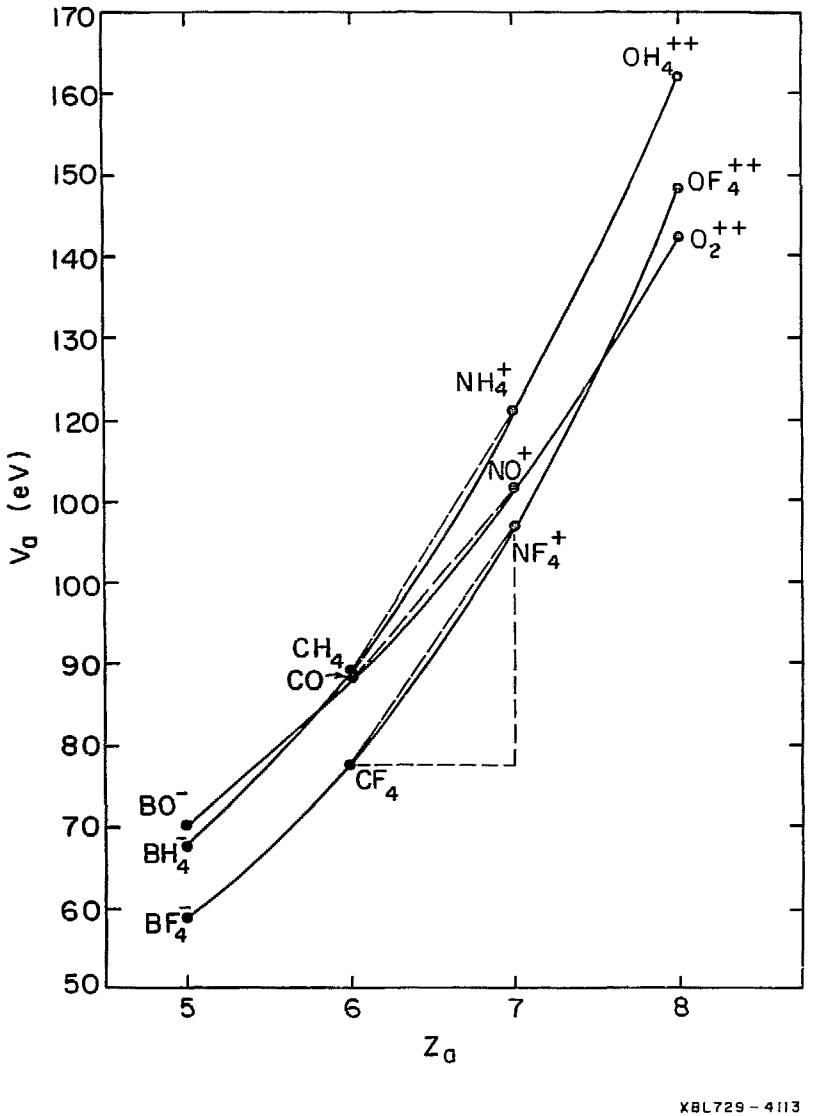

XBL729-4113

Fig. 4. V_a is plotted against Z_a for three different isoelectronic molecular systems. The linear relaxation energy for a C 1s transition from CF_4 is the area within the dotted lines.

$$\psi_i = \sum_j c_{ij}\, \phi_j \quad ,$$

where the ϕ's are atomic orbitals. The c_{ij}'s must satisfy the normalization condition imposed on the ψ_i's -- $\int \psi^* \psi \, d\tau = 1$, or

$$\sum_j \sum_k (c_{ij}\, c_{ik}^* \int \phi_j\, \phi_k^* \, d\tau) = 1 \qquad (10)$$

In the calculation of CNDO/2 wavefunctions, it is assumed that $\int \phi_j\, \phi_k^* \, d\tau = \delta_{jk}$ so that the normalization condition reduces to $\sum_j c_{ij}\, c_{ij}^* = 1$. The CNDO/2 molecular orbitals are real, so Eq. (10) becomes

$$\sum_j c_{ij}^2 = 1 \quad .$$

An analogous approximation to that of assuming $\int \phi_j\, \phi_k^* = \delta_{jk}$ is used when calculating $V_a(Z)$ with CNDO/2 wavefunctions. Now $V_a(Z)$ is given by the expectation value

$$\int \Psi \left(\sum_i^n \frac{e^2}{r_{ia}} \right) \Psi \, d\tau_1 .. d\tau_n - \sum_{j \neq a} \frac{e^2 Z_j}{r_{ja}} \quad ,$$

where Ψ represents $\Psi(1...n)$, and n is the total number of electrons; the part of V_a which depends on the electrons will be called V_a^e. Because $1/r_{ia}$ is a one-electron operator, and the molecular orbitals are assumed to be orthogonal, one gets for V_a^e, in the <u>molecular orbital approximation</u>,

$$V_a^e(Z_a) = \sum_i^n \int \psi_i(i) \, \frac{e^2}{r_{ia}} \, \psi_i(i) \, d\tau_i \quad .$$

And since $\psi_i(i) = \sum_j c_{ij}\, \phi_j(i)$, $V_a^e(Z)$ becomes

$$V_a^e = \sum_i^n \sum_j \sum_k c_{ij}\, c_{ik} \int \phi_j(i)\, (e^2/r_{ia})\, \phi_k(i)\, d\tau_i \quad .$$

This expression for V_a will now be broken up into several parts in order to point out the most important parts and to make some approximations. First, let the atomic orbitals which are centered at atom a be labeled ϕ_j^a. If Slater[44] atomic orbitals are used, and the orbitals have the same principal quantum number,

$$\int \phi_j^a(i)\, (e^2/r_{ia})\, \phi_k^a(i)\, d\tau_i = V_a^a\, \delta_{jk} \quad .$$

V_a^a is, of course,

$$\int \phi_j^a(i)\, (e^2/r_{ia})\, \phi_j^a(i)\, d\tau_i \quad .$$

With this notation, V_a^e becomes

$$V_a^a \left(\sum_i \sum_j c_{ij}^{a\,2} \right) + \sum_i \sum_j c_{ij}^{b\,2} \left(\int \phi_j^b(i)\, \frac{e^2}{r_{ia}}\, \phi_j^b(i)\, d\tau_i \right)$$

$$+ \sum_i \sum_j \sum_k c_{ij}^b\, c_{ik}^c \int \phi_j^b(i)\, \frac{e^2}{r_{ia}}\, \phi_k^c(i)\, d\tau \quad .$$

$$j \neq k$$

In this notation, b refers to atoms other than a, while c refers to any atom. The first term is the dominant one for V_a^e; the double sum in the

first term is closely related to the number of electrons near atom a, and is called the net electronic population at atom a. V_a^a varies between 15 eV and 40 eV along the first row elements, from boron to neon. The second term involves two-center integrals (atoms a and b), but only one atomic orbital (centered on atom b). These integrals are at most one-half of V_a^a; obviously they are largest when atom b is bonded to atom a. These two-center integrals vary with R_{ab} approximately as $1/R_{ab}$; in fact, if the atomic orbital is an s orbital, the integral in atomic units is exactly $1/R_{ab}$.

The third term involves two- and three-center integrals, in which the atomic orbitals are not on the same center. All of these integrals will be neglected here (except those needed to preserve the invariance of V_a to coordinate transformations; this point will be discussed in more detail later). This is a very sizable approximation; when the centers are adjacent to each other, two-center integrals are comparable to the largest integrals in the second term. A partial justification for this approximation is the following: consider for simplicity a homonuclear diatomic molecule, and a molecular orbital $\psi_i = c\phi_a \pm c\phi_b$. In the CNDO approximation, c^2 must be 0.5, because it is assumed that $\int_{\tau_i} \psi_i^2 = 1$ and $\int \phi_a \phi_b \, d\tau = 0$. However, for realistic orbitals, the normalization condition demands that $c^2 = .5/(1 \pm \int \phi_a \phi_b \, d\tau)$. Now in most cases, $\int \phi_a \phi_b = 0.1$ to 0.3, so this is a sizable approximation, leading to a change in the one center part of the potential (the first term) of several eV, due to the CNDO/2 net electronic population (which depends on c^2) being too large or too small, depending on whether the sign is + or - in the molecular orbital. However, there is a corresponding integral in the third

term, whose neglect compensates for the error in the CNDO net atomic population; this integral is in a term of the form $\pm c^2 \int \phi_a \, 1/r_{ia} \, \phi_b \, d\tau_i$ which is also several eV. The two errors will always be of opposite sign, and because the neglected two-center integral is roughly proportional to the overlap integral (see Fig. 5), the two errors will cancel in large measure. However, the cancellation is only approximate, and therefore the resultant error in V_a can be of the order of electron volts. In addition to these errors, there is an error in V_a due to the use of semi-empirical wavefunctions rather than ab initio ones. This error seems to be small, however, by comparison of the CNDO/2 chemical shifts with those obtained from ab initio wavefunctions.[25]

Two approaches were used to calculate V_a; in one approach, integrals not neglected were calculated exactly using formulas due to Roothaan;[23] in another, the two-center integrals were approximated by $1/R_{ab}$. The first approach gives substantially better agreement with experiment, but the second approach is more intuitively appealing. In the second approach, V_a becomes

$$V_a^a P_a - \sum_{j \neq a} e^2 q_j / R_{ja} \qquad P_a = \text{net electronic population at atom } a,$$

where q_j is the net charge on atom j. q_j is the difference between the net electronic population and the nuclear charge. Thus the second approach is a "point-charge" model of the electronic charge distribution in the molecule. In such a model, the chemical shifts determine linear equations involving the net atomic charges.† If enough chemical shifts are measured,

†It is assumed here that $\Delta R = 0$; $\Delta E_B = -\Delta V_a$.

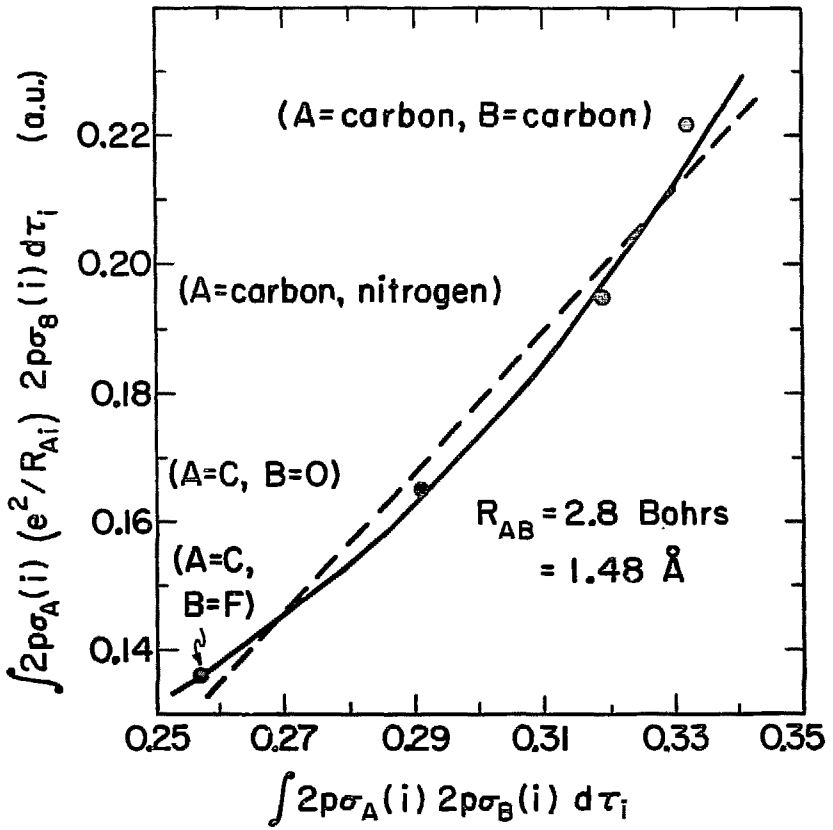

XBL735-2836

Fig. 5. Two-center matrix elements of R_{AB}^{-1} are plotted against the corresponding two-center matrix elements of the overlap for various nuclei.

the linear equations may be solved for the atomic charges; thus the atomic charges so obtained are strictly empirical. This approach will be discussed later.

Siegbahn, et al.[6] have correlated chemical shifts well with changes in a CNDO/2 point-charge model potential. They varied V_a^a to maximize the correlation. With this model, of course, they did not consider possible changes in R, the relaxation energy.

Getting back to the first approach, its exact calculation of the two-center integrals takes into account the differences between 2s, 2pσ, and 2pπ orbitals. These differences are fairly large; for a C_2 molecule and an internuclear distance of 1.5 Å, they are, respectively, 9.60 eV, 10.77 eV, and 9.01 eV. It should be noted that in the first approach the two-center part of the potential depends on both the magnitude of the net electronic population and how it is partitioned among the various atomic orbitals; in the point charge model, all the orbitals are treated as if they were s orbitals, so the partitioning makes no difference to the point charge potential. Thus the first model should be more sensitive to changes in chemical environment than the point charge model. For example, Siegbahn, et al.[6] point out that the point-charge model cannot explain the nitrogen and oxygen chemical shifts between NO, N_2, and O_2, because the core electrons in NO have higher binding energies than those in either N_2 or O_2. However, because of its greater flexibility, the first model does reproduce this effect.

As mentioned previously, some of the elements in the third term of V_a are retained in the first model. These elements have the form

$$c_{ij}\, c_{ik} \int \phi^{b}_{2p}\, 1/r_{ia}\, \phi^{b}_{2p'}\, d\tau_i \quad .$$

The atomic orbitals within the integral are 2p orbitals of different magnetic quantum number, and centered on the same atom. These "non-diagonal" matrix elements are of the order of 0 to 0.2 eV, so they don't contribute substantially to the potential; however, they are necessary if V_a is to have the same symmetry as the nuclear framework of the molecule. Originally, these "non-diagonal" elements were left out, and as a consequence symmetrically equivalent nuclei were found to have different potentials in certain cases. It is difficult to explain this effect in a few words--what it takes is a good visualization of the 2p atomic orbitals in different orientations--but roughly the reason for this effect is that a definite coordinate system must be chosen in which to define the orientation of the p orbitals. Therefore, the diagonal matrix elements of the two-center integrals for atoms a and b may vary with the direction of R_{ab}. This concludes the discussion of the calculation of V_a. The calculation of CNDO/2 wavefunctions has been developed by Pople, and is discussed in detail by Pople and Beveridge.[24]

Two models were used to predict core-level shifts with V_a and CNDO/2 wavefunctions:

$$\Delta E^{e}_{B} = -\Delta V_a$$

$$\Delta E^{e}_{B} = -\Delta V_a - \Delta R_a \quad ,$$

where $R_a = 1/2(V_a(Z^0_a + 1) - V_a(Z^0_a))$. The first potential model was used for the calculation of V_a for most molecules because it generally gives

better agreement with experiment; this is shown for the fluoromethanes in Fig. 6. From now on, the first potential model will be called the pp' model because of the off-diagonal matrix elements employed in it.

The first model is preferable to chemists because with it, experimental chemical shifts can be interpreted in terms of ground-state wavefunctions. However, ΔR must be zero, or close to zero for the first approach to be valid. To test this, a table of relaxation energies, R, was calculated with CNDO/2 wavefunctions; in Table III, the relaxation energies are listed in order of their magnitude.

D. The Problem of Relaxation

It would be useful to have a thorough comparison of the relaxation energies calculated by CNDO/2 with those calculated by ab initio wavefunctions. At the present time, however, only a few values of ab initio relaxation energies have been published.[26] The relaxation approach usually but not always[26] works as well or better (it should always work better) than the ground state approach to chemical shifts with CNDO/2 wavefunctions. Also, the CNDO/2 results exaggerate the ab initio result for $R_c(CH_4) - R_c(CO)$ by about 2 eV. Another notable failure of the CNDO/2 relaxation approach is its exaggeration of the chemical shifts between C_6H_6 and the compounds C_2H_4 and CH_4. Because of the very similar electronegativity of carbon and hydrogen, these compounds are expected to have similar values for the ground state potential at the carbon nucleus (CNDO/2 values are 88.88, 88.89, and 88.31 eV for CH_4, C_2H_4, and C_6H_6). Therefore, the carbon shifts should depend heavily on differences in the relaxation energy. The experimental

Table III. Relaxation Energies

Molecule	Carbon Nuclei R (eV) (R = 1/2($V_a(Z^0 + 1) - V_a(Z^0)$))
CO	11.92
CO_2	12.86
HCN	14.40
CF_4	14.91
HCOOH	15.31
CF_3H	15.38
C_2H_4	15.43
C_2H_2	15.58
CF_2H_2	15.73
CH_4	15.89
CFH_3	15.92
$C^*F_3CH_2OH$	15.93
$C^*F_3CH_2NH_2$	16.00
$H_3C - C^*F_2H$	16 11
CH_3OH	16.13
$CF_3 - CF_3$	16.19
$H_2C = C^*F_2$	16.25
$H_3C - C^*FH_2$	16.30
$C^*F_3 - CF_2 - CF_3$	16.42
$CF_3^* - CF = CF - CF_3$	16.42
$CH_3 - CH_3$	16.50
$CH_2 = C^*HF$	16.52

(continued)

Table III. (continued)

Molecule	Carbon Nuclei	R (eV) ($R = 1/2(V_a(Z^0 + 1) - V_a(Z^0))$
$C^*H_3 - CH_2F$		16.53
$H_2C\overset{O}{\diagup\!\!\diagdown}CH_2$		16.53
$CHF = CF_2$		16.58
$CH_3CH_2NH_2$		16.65
$C^*H_3 - CHF_2$		16.71
$C^*H_3 - CF_3$		16.75
$C^*H_2 = CHF$		16.88
$(C^*H_3)_2CHNO_2$		16.93
$CF_3C^*H_2OH$		16.94
$C^*HF = CF_2$		16.96
$C^*H_2 = CF_2$		16.99
CH_3NO_2		16.99
$CH_3 - C^*F_3$		15.86
$CF_3 - CF_2 - CF_3$		17.30
cyclo $C_6H_3F_3$ (C_F carbon)		17.43
$(CH_3)_2C^*HNO_2$		17.57
cyclo C_4F_6 (CF_2 carbon)		17.63
cyclo C_4F_8		17.65
cyclo $C_6H_4F_2$ (C_F carbon)		17.65
cyclo C_6H_6 (benzene)		17.69
cyclo $C_6H_4F_2$		17.80

(continued)

Table III. (continued)

Molecule	R (eV) ($R = 1/2(V_a(Z^0 + 1) - V_a(Z^0))$)
Carbon Nuclei	
$CF_3C^{*}F = CFCF_3$	17.86
cyclo $C_6F_3H_3$ (C_H carbon)	17.94
cyclo C_6F_6	17.95
cyclo C_4F_6 (CF carbon)	17.97
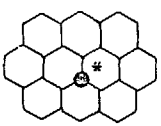 (graphite)	19.14
Nitrogen Nuclei	
NO	15.73
N_2	16.67
HCN	18.50
NH_3	19.01
NF_3	19.32
CH_3NH_2	19.75
$H_2N - NH_2$	19.98
NF_2	20.00
CH_3NO_2	20.00
NO_2	20.39
$(CH_3)_2CHNO_2$	20.47
$C_6H_5NO_2$	20.61

(continued)

Table III. (continued)

Molecule	R (eV) ($R = 1/2(V_a(Z^0 + 1) - V_a(Z^0))$)
Nitrogen Nuclei	
NOF_3	20.63
N_2F_4	22.99
Oxygen Nuclei	
O_2	14.38
NO	20.35
NO_2	20.35
H_2O	20.63
CO	21.46
NNO	22.02
CH_3OH	22.18
CF_3CH_2OH	22.63
$HC = O^* - OH$	22.36
CH_3CH_2OH	22.66
$> C\underline{-O-}C <$	22.82
CH_3NO_2	23.14
$HC = O - OH^*$	23.30
$(CH_3)_2CHNO_2$	23.54
$C_6H_5NO_2$	23.79
$(CH_3CH_2)_2O$	24.16
cyclo C_4H_4O (furan)	24.27

shifts are, relative to CH_4, -0.1 eV for C_2H_4 and -0.4 eV for C_6H_6, so that R should not vary by more than 1 eV for these compounds; the CNDO/2 relaxation energies give ΔR_c between C_6H_6 and CH_4 as 1.80 eV, and between C_6H_6 and C_2H_4 as 2.26 eV. With this in mind, the CNDO/2 relaxation energies should be viewed in a qualitative sense, rather than a quantitative one.

The list of relaxation energies in Table III exhibits some definite trends with molecular structure; the most obvious one is the increase in R with the number of atomic centers in the molecule. A related trend is the increase in R as ligands are added to an atom. Another trend is the decrease in R with the substitution of F for H in a chemical bond. A fourth trend is for atoms in an unsaturated or cyclic system to have high values of R.

The first two trends can be partly explained by Coulomb's law, following an argument given by D. A. Shirley:[27] Relaxation always involves the movement of electronic charge toward an ionized atom from other atomic centers; Coulomb's law implies that as one removes electronic charge from another center, the energy required for this goes up with the amount of charge already removed. Therefore, as more centers become available, less charge is removed from any one center, and the ion becomes more energetically stable. This effect is so important that it may actually limit the amount of charge moved toward the ionized atom, as in the case of diatomic molecules.[26]

The reluctance of the fluorine atom to give up electronic charge to an ionized neighbor may be a consequence of its greater electronegativity, while the relatively high values of R for conjugated and cyclic systems may result from the high electronic density throughout the

molecule in the ground state; because of Coulomb's law, a higher density of electrons would stabilize a positive charge (inner shell vacancy) more than a lower density.

E. Discussion of Results

The implication of the above for chemists is that R must be considered in order to interpret chemical shifts correctly--the total range of R is 7 eV for carbon, while the total range of chemical shifts is about 12 eV. However, it may be possible to find classes of molecules for which ΔR is close to zero, so that one may apply the ground state model with confidence. With this in mind, the CNDO/2 ground state approach has been applied to a number of molecules without regard to differences in R, and then to several series of molecules without regard to differences in R, and then to several series of molecules separately on the basis of the table of relaxation energies and chemical similarity. Whereas the "blanket" application predicts shifts to within no better than 1 eV on the average, the restriction of the ground-state model to separate classes of molecules gives substantially better results--usually these predictions are good to 0.3 or 0.4 eV. The "blanket" approach and the restricted approach are illustrated in Figs. 6 to 12. The classes of molecules include the fluoromethanes, the fluoroethanes, the fluoroethylenes, oxygen atoms bonded to only one other atom, oxygen atoms bonded to two other atoms, and fluorine atoms (all of which are bonded to only one other atom). There was no large group of nitrogen binding energies for which the ground state approach held with accuracy. The N_2 - NO and H_2NNH_2 - F_2NNF_2 chemical shifts were predicted well, while the

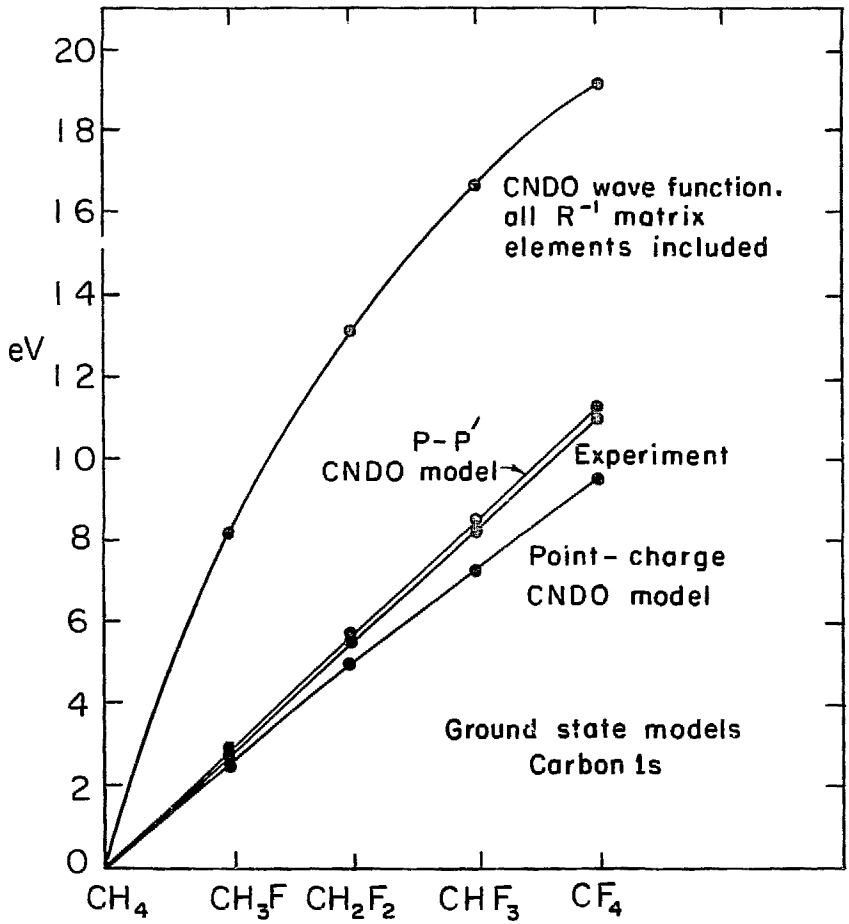

XBL7210-4[illegible]

Fig. 6. Various ground state potential models using CNDO/2 wavefunctions are compared with experiment.

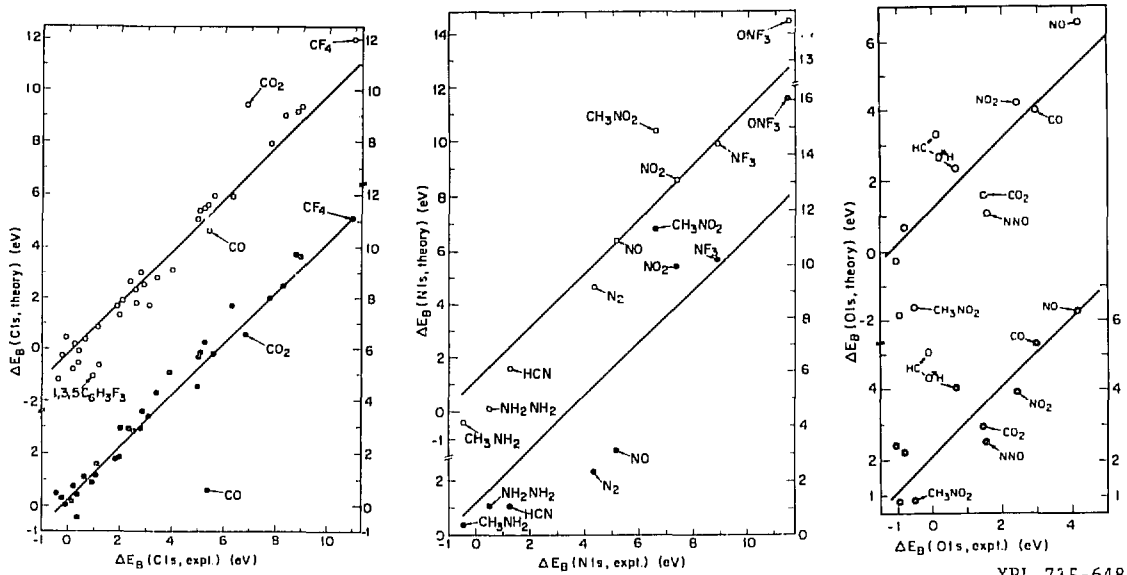

XBL 735-648

Fig. 7. This illustrates the "blanket" approach toward predicting chemical shifts. Both the ground state model (in filled circles) and the relaxation model (in open circles) are presented. The lines represent best least-squares fits of experiment to theory under the constraint of unit slope. The standard deviations are given in Ref. 26.

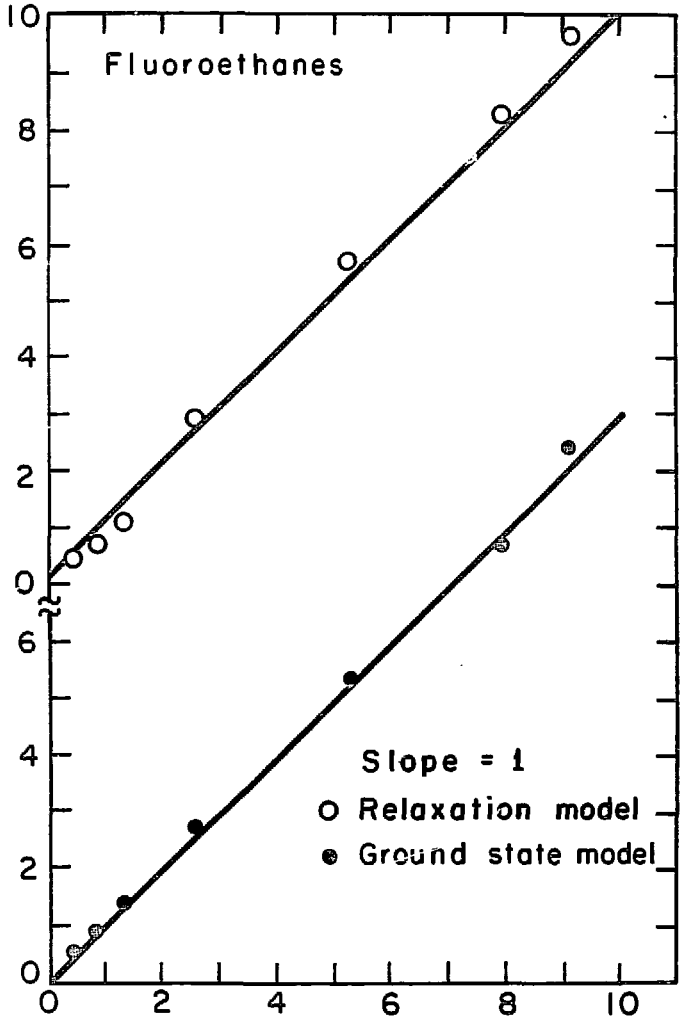

XBL727-3617

Fig. 8. Both CNDO/2 potential models are compared with experiment for the carbon chemical shifts in the fluoroethanes. The standard deviation for the ground state model is 0.14 eV and 0.31 eV for the relaxation model.

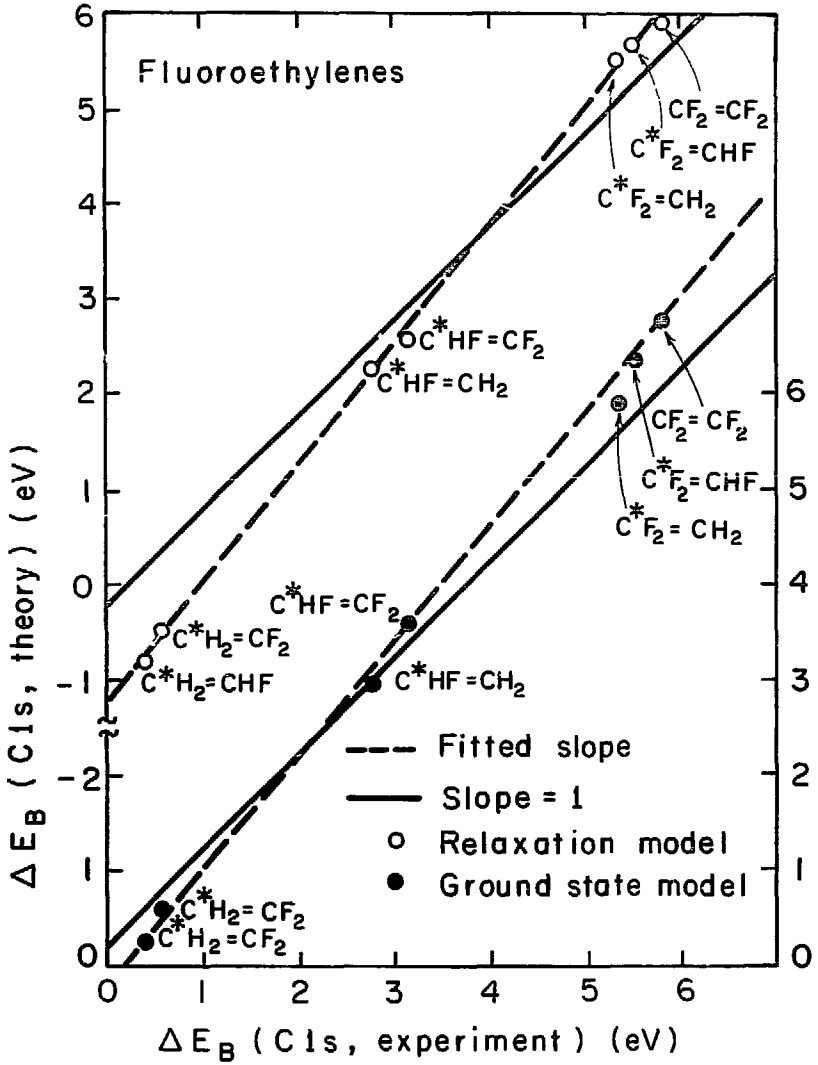

XBL727-3559

Fig. 9. Same as Fig. 8, except that it illustrates C 1s shifts in the fluoroethylenes. For a slope equal to one, the standard deviation is 0.38 eV for the ground state model and 0.53 eV for the relaxation model. For the fitted slope, the corresponding standard deviations are 0.12 eV and 0.07 eV. For the ground state model, the fitted slope is 1.17, and for the relaxation model, it is 1.25.

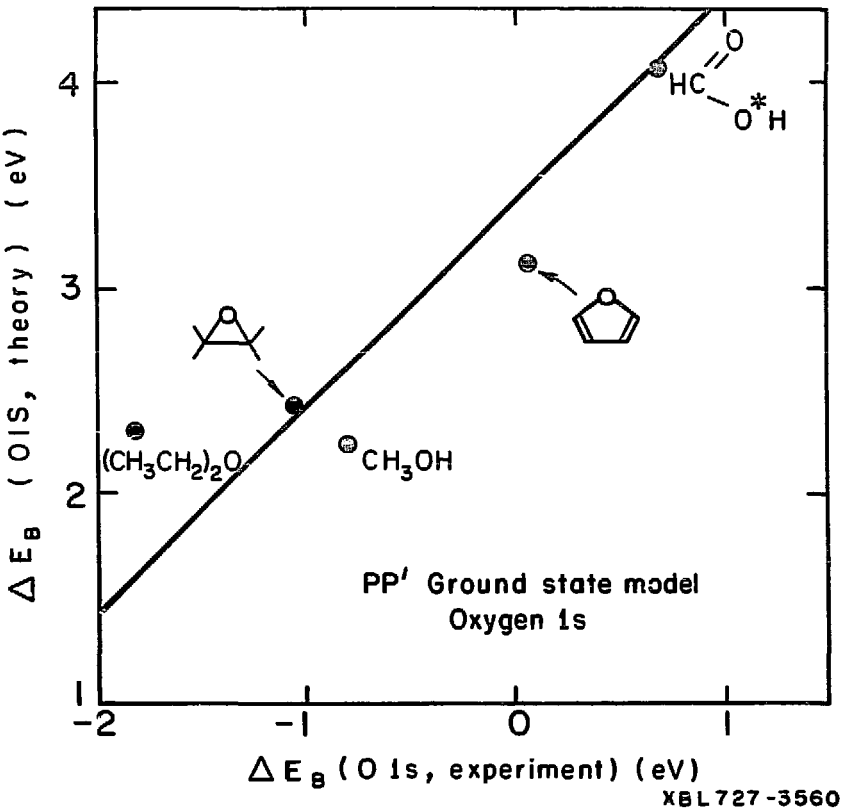

Fig. 10. Same as Fig. 8, except that it illustrates oxygen 1s shifts for oxygen atoms bonded to one other atom. The standard deviation is 0.35 eV.

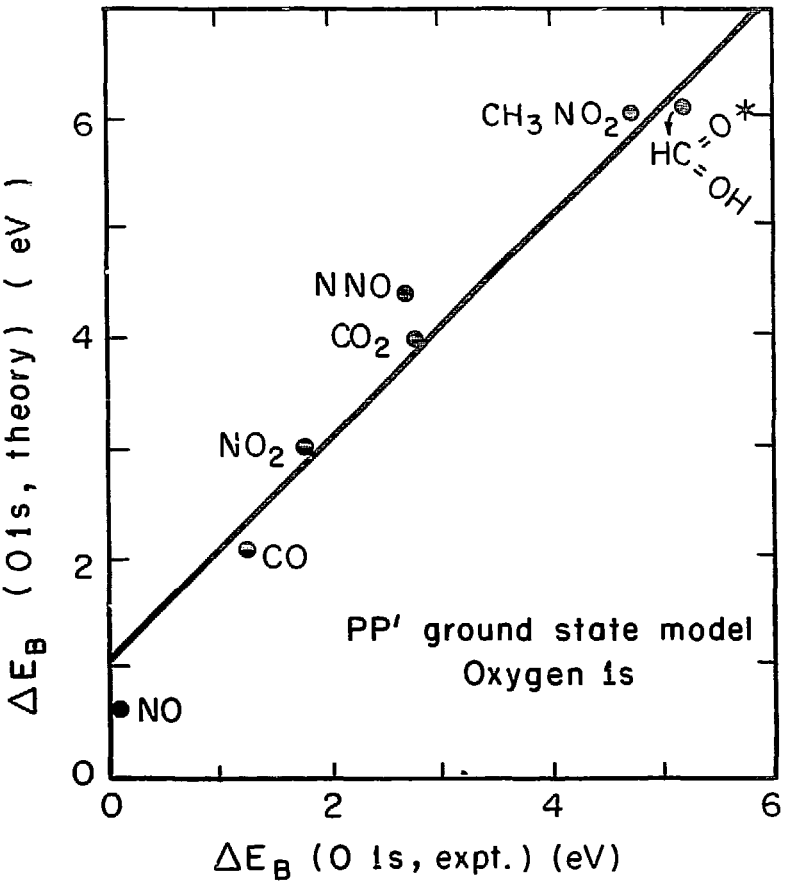

XBL727-3419

Fig. 11. Same as Fig. 8, except that it illustrates oxygen 1s shifts for oxygen atoms bonded to two other atoms. The standard deviation is 0.40 eV.

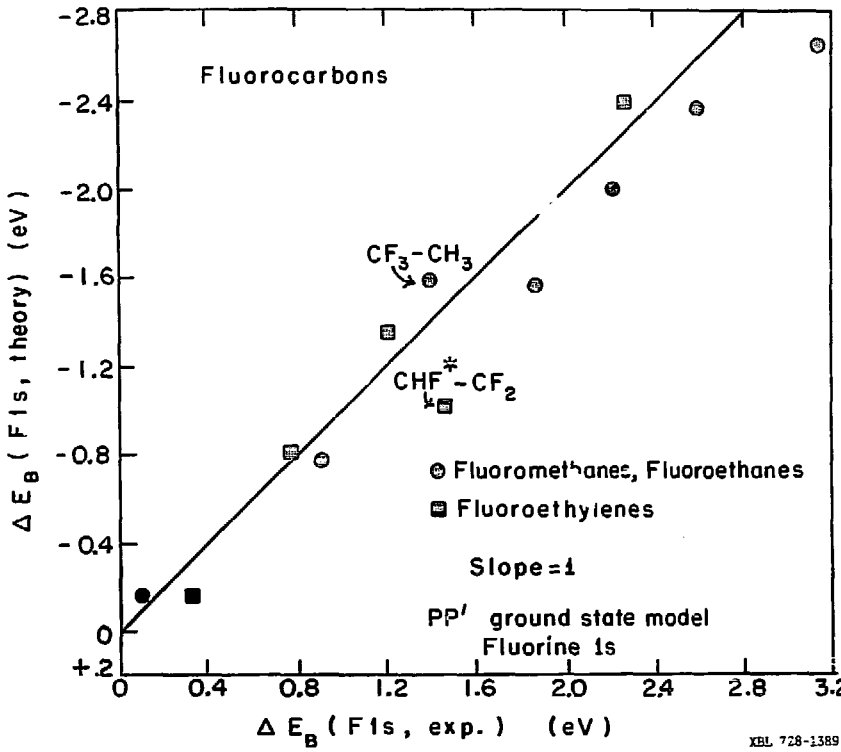

Fig. 12. Same as Fig. 8, except that it illustrates fluorine 1s shifts in fluorocarbons. The standard deviation is less than 0.4 eV.

NH_3 - NF_3 chemical shifts was exaggerated by about 1 eV. In fact, the case of the nitrogen binding energies is the only one where the CNDO/2 relaxation model gives substantial improvement over the ground state approach. The CNDO/2 potentials are listed in Table V; the experimental chemical shifts measured here are listed in Table IV.

The success of the CNDO/2 potential models lends credence to the CNDO/2 charge distributions--obviously, the potential at a nucleus depends heavily on the charge distribution in the molecule. In particular, the CNDO/2 method predicts electronegative substituents to polarize molecules in a very definite manner: the atomic charges obtained from CNDO/2 wavefunctions tend to alternate in sign as one proceeds away from the substituent. For example, the CNDO/2 method predicts the β-carbons in α-fluorinated ethanes to have negative charges, e.g.,

$$F_3C - CH_3 \quad .$$

This type of charge distribution was tested further; one of the hydrogens on the β-carbon in CF_3CH_3 was replaced by the electronegative group - NH_2. If the CNDO/2 charge distribution were correct, this group would tend to decrease the positive charge on the α-carbon in CF_3CH_3 and perhaps even lower its core binding energy. This did occur--the binding energy of the CF_3 carbon in $CF_3CH_2NH_2$ was lower by 0.2 eV than the CF_3 carbon in CF_3CH_3. The CNDO/2 potential models predicted the shift correctly also, although they indicate that much of the shift between the CF_3 carbons is due to relaxation. The oxygen 1s shift between CF_3CH_2OH and CH_3CH_2OH was also predicted exactly by the CNDO/2 ground state potential model. In this

Table IV. CNDO/2 Potential Energies (eV), PP' Model

Molecule	$V_a(Z^0)$	$V_a(Z^0 + 1)$	$-\Delta V_a(Z^0)$	$-\Delta[1/2(V_a(Z^0) + V_a(Z^0 + 1))]$
		Carbon Nuclei		
CH_4	88.88	120.65	0	0
CH_3F	85.89	117.73	2.99	2.96
CH_2F_2	83.06	114.52	5.82	5.96
CHF_3	80.34	111.10	8.54	9.05
CF_4	77.75	107.56	11.13	12.11
C_2H_6	88.54	121.53	0.34	-0.27
$CH_3^* - CH_2F$	88.10	121.15	0.78	0.14
$CH_3 - C^*H_2F$	85.82	118.42	3.06	2.65
$CH_3^* - CHF_2$	87.70	121.12	1.18	0.36
$CH_3 - CHF_2$	83.22	115.44	5.66	5.44
$CH^*_3 - CF_3$	87.18	120.68	1.70	0.85
$CH_3 - C^*F_3$	80.84	112.56	8.04	8.01
$CF_3 - CF_3$	79.18	111.56	9.70	9.40
$CF_3 - C^*F_2 - CF_3$	80.93	115.52	7.95	6.54
$CF_3 - CF_2 - C^*F_3$	79.11	111.94	9.77	9.24

(continued)

Table IV. (continued)

Molecule	$V_a(Z^0)$	$V_a(Z^0 + 1)$	$-\Delta V_a(Z^0)$	$-\Delta[1/2(V_a(Z^0) + V_a(Z^0 + 1))]$
		Carbon Nuclei		
cyclo C_4F_8	81.16	116.45	7.72	5.96
$CH_2 = CH_2$	88.89	119.74	-0.01	+0.45
$CH^*_2 = CHF$	88.66	122.42	0.22	-0.78
$CH_2 = C^*HF$	85.93	118.97	2.95	2.22
$CH^*_2 = CF_2$	88.30	122.28	0.50	-0.53
$CH_2 = C^*F_2$	83.02	115.51	5.86	5.50
$C^*HF = CF_2$	85.28	119.20	3.60	2.53
$CHF = C^*F_2$	82.57	115.73	6.31	5.62
$CF_2 = CF_2$	82.15	115.53	6.65	5.88
CH = CH	89.27	120.42	-0.39	-0.08
cyclo C_6H_6	88.31	123.68	0.57	-1.23
cyclo $C_6H_4F_2$	87.63	123.23	1.25	-0.67
cyclo $C_6H_4F_2$	85.40	120.70	3.48	1.72
cyclo $C_6F_3H_3$	87.91	123.79	0.97	-1.09
cyclo $C_6F_3H_3$	84.50	119.36	4.38	2.84

(continued)

Table IV. (continued)

Molecule	$V_a(Z^0)$	$V_a(Z^0 + 1)$	$-\Delta V_a(Z^0)$	$-\Delta[1/2(V_a(Z^0) + V_a(Z^0 + 1))]$
		Carbon Nuclei		
cyclo C_6F_6	83.68	119.58	5.20	3.14
HCN	88.57	117.36	0.31	1.80
CH_3NO_2	85.87	119.86	3.01	1.91
CO	88.21	112.03	0.67	4.65
CO_2	82.31	108.02	6.57	9.60
HCOOH	84.37	114.98	4.51	5.09
CH_3OH	87.01	119.27	1.87	1.63
cyclo C_2H_4O	86.95	120.01	1.93	1.29
$(C^*H_3)_2CHNO_2$	87.50	121.35	1.38	0.34
$(CH_3)_2C^*HNO_2$	85.79	120.92	3.09	1.41
cyclo C_4F_6	84.03	119.96	4.85	2.77
cyclo C_4F_6	80.85	116.10	8.03	6.29
per-fluoro-2 butene	83.52	119.24	5.36	3.39
per-fluoro-2 butene	79.53	112.36	9.35	8.82

(continued)

Table IV. (continued)

Molecule	$V_a(Z^0)$	$V_a(Z^0 + 1)$	$-\Delta V_a(Z^0)$	$-\Delta[1/2(V_a(Z^0) + V_a(Z^0 + 1))]$
Carbon Nuclei				
$C^{*}F_3 - CH_2NH_2$	80.89	112.88	7.99	7.88
$C^{*}H_3CH_2NH_2$	88.65	121.94	0.23	-0.54
Nitrogen Nuclei				
N_2	133.22	166.56	2.32	4.66
NO	132.43	163.89	3.11	6.39
NO_2	125.58	166.36	9.96	8.58
CH_3NO_2	124.22	164.22	11.32	10.33
HCN	134.47	171.46	1.07	1.59
NH_3	135.54	173.56	0	0
CH_3NH_2	135.17	174.67	0.37	-0.38
NF_3	125.34	163.98	10.20	9.89
$H_2N - NH_2$	134.46	174.41	1.08	0.12
NOF_3	119.46	160.71	16.08	14.47
N_2F_4	127.76	173.73	7.78	3.81

(continued)

Table IV. (continued)

Molecule	$V_a(Z^0)$	$V_a(Z^0 + 1)$	$-\Delta V_a(Z^0)$	$-\Delta[1/2(V_a(Z^0) + V_a(Z^0 + 1))]$
		Nitrogen Nuclei		
$C_6H_5NO_2$	125.04	166.26	10.51	8.91
NF_2	131.24	171.35	4.3	3.25
$(CH_3)_2CHNO_2$	124.67	165.61	10.87	9.41
$CH_3CH_2NH_2$	135.24	--	0.30	--
$CF_3CH_2NH_2$	134.25	--	1.29	--
		Oxygen Nuclei		
H_2O	192.22	233.47	0.0	0.0
O_2	185.30	214.06	6.92	13.17
CO	187.39	230.31	4.83	4.00
NO	185.94	226.63	6.28	6.56
NO_2	188.29	228.98	3.93	4.21
CH_3NO_2	191.33	237.60	0.89	-1.62
$HCOO^{\#}H$	188.16	232.88	4.06	2.33
$HCO^{\#}OH$	191.38	237.97	0.84	-1.83

(continued)

Table IV. (continued)

Oxygen Nuclei

Molecule	$V_a(Z^0)$	$V_a(Z^0 + 1)$	$-\Delta V_a(Z^0)$	$-\Delta[1/2(V_a(Z^0) + V_a(Z^0 + 1))]$
CH_3OH	189.97	234.32	2.25	0.70
C_2H_4O	189.79	235.42	2.43	-0.24
$C_6H_5NO_2$	191.88	239.45	0.34	-2.82
NNO	189.69	233.73	2.53	1.09
$(CH_3CH_2)_2O$	189.92	238.24	2.30	-1.24
C_4H_4O	189.10	237.64	3.12	-0.53
$(CH_3)_2CHNO_2$	191.58	238.65	0.64	-0.23
CH_3CH_2OH	190.12	235.44	2.10	0.07
CF_3CH_2OH	188.81	234.06	3.41	1.42

Fluorine Nuclei

Molecule	$V_a(Z)$	$-\Delta V_a(Z)$
CF_4	249.85	0.
CH_3F	252.19	-2.34
CH_2F_2	251.40	-1.55
CHF_3	250.62	-0.77

(continued)

Table IV. (continued)

Molecule	Fluorine Nuclei $V_a(Z)$	$-\Delta V_a(Z)$
CH_3CH_2F	252.50	-2.65
CH_3CHF_2	251.84	-1.99
CH_3CF_3	251.42	-1.57
$CF_3CF_2CF_3^*$	249.52	+0.33
$CF_3CF_2^*CF_3$	249.68	+0.17
cyclo C_4F_8	249.70	+0.15
$CH_2 = CHF$	251.93	-2.08
$CH_2 = CF_2$	251.18	-1.33
$CHF^* = CF_2$	250.65	-0.80
$CHF = CF_2^*$	250.00	-0.15
cyclo C_4F_6	249.96	-0.11
	250.49	-0.64
$CF_3(F)C = C(F)CF_3$	250.08	-0.23
	250.24	-0.39

Table V. Experimental Chemical Shifts

Compound	Reference	Core Level	E_B(Ref) - E_B(compound) (eV)
C_6H_6	CF_4	C 1s	-11.54 ± 0.02
CHF_3	CF_4	C 1s	-2.72 ± 0.03
CH_2F_2	CF_4	C 1s	-5.52 ± 0.04
CH_2F_2	CF_4	F 1s	-1.83 ± 0.1
CH_3CH_3	CF_4	C 1s	-11.20 ± 0.04
CH_3CH_2F	CF_4	C 1s	-8.57, -10.77 ± 0.05
CH_3CH_2F	CF_4	F 1s	-3.20 ± 0.06
CH_3CHF_2	CF_4	C 1s	-5.91, 10.34 ± 0.04
CH_3CHF_2	CF_4	C 1s	-2.22 ± 0.06
CH_3CF_3	CF_4	C 1s	-3.32, -9.89 ± 0.06
CH_3CF_3	CF_4	F 1s	-1.40 ± 0.2
CF_3CF_3	CF_4	C 1s	-2.11 ± 0.06
CF_3CF_3	CF_4	F 1s	-0.19 ± 0.1
$CF_3CF_2CF_3$	CF_4	C 1s	-2.22, -4.22, ±0.03
$CF_3CF_2CF_3$	CF_4	F 1s	-2.45, -0.91 ± 0.2
$CF_3CH_2NH_2$	CF_4	C 1s	-3.54, -9.19 ± 0.06
$CF_3CH_2NH_2$	CF_4	F 1s	-1.45 ± 0.2
$CF_3CH_2NH_2$	N_2	N 1s	-4.07 ± 0.04
$CH_3CH_2NH_2$	N_2	N 1s	-4.93 ± 0.04
CH_3CH_2OH	O_2	O 1s	-4.63 ± 0.06
CF_3CH_2OH	O_2	O 1s	-3.51 ± 0.04
CF_3CH_2OH	CF_4	C 1s	-3.25, -9.19 ± 0.06
CF_3CH_2OH	CF_4	F 1s	-1.09 ± 0.2

(continued)

Table V. (continued)

Compound	Reference	Core Level	E_B(Ref) - E_B(compound) (eV)
$(CF_3)_3COH$	CF_4	C 1s	-6.93, -2.50 ± 0.2
$(CF_3)_3COH$	O_2	O 1s	-2.63 ± 0.06
$H_2C = CH_2$	CF_4	C 1s	-11.1 ± 0.2 (a)
$H_2C = CHF$	CF_4	C 1s	-8.48, -10.86 ± 0.1
$H_2C = CHF$	CF_4	F 1s	-2.26 ± 0.1
$H_2C = CF_2$	CF_4	C 1s	-5.86, -10.63 ± 0.03
$H_2C = CF_2$	CF_4	F 1s	-1.08 ± 0.1
$CHF = CF_2$	CF_4	C 1s	-5.71, -8.09 ± 0.04
$CHF = CF_2$	CF_4	F 1s	-0.72, -1.42 ± 0.2
$CF_2 = CF_2$	CF_4	C 1s	-5.42 ± 0.04
$CF_2 = CF_2$	CF_4	F 1s	-0.50 ± 0.2
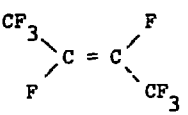	CF_4	C 1s	-2.27, -7.04 ± 0.05
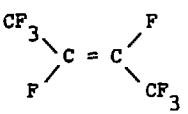	CF_4	C 1s	-0.56, -0.98 ± 0.2
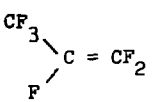	CF_4	C 1s	-2.36, -4.98, -7.28 ± 0.1
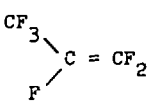	CF_4	F 1s	-0.31, -0.72, -1.28 ± 0.3
$CF_3CH = CH_2$	CF_4	C 1s	-3.24, -9.93, -10.40 ± 0.1

(continued)

Table V. (continued)

Compound	Reference	Core Level	E_B(Ref) - E_B(compound) (eV)
$CF_3CH = CH_2$	CF_4	F 1s	-1.40 ± 0.2
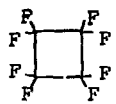	CF_4	C 1s	-4.71 ± 0.05
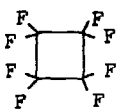	CF_4	F 1s	-0.44 ± 0.2
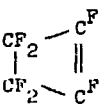	CF_4	C 1s	-2.31, -4.77 ± 0.07
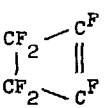	CF_4	F 1s	-0.694, -1.49 ± 0.2
CH_3NO_2	CF_4	C 1s	-8.92 ± 0.05
CH_3NO_2	N_2	N 1s	2.23 ± 0.04
CH_3NO_2	O_2	O 1s	-3.98 ± 0.04
$(CH_3)_3CHNO_2$	CF_4	C 1s	-9.35, -10.53 ± 0.1
$(CH_3)_3CHNO_2$	N_2	N 1s	1.58 ± 0.03
$(CH_3)_3CHNO_2$	O_2	O 1s	-4.36 ± 0.03
$C_6H_5NO_2$	N_2	N 1s	+1.80 ± 0.04
$C_6H_5NO_2$	O_2	O 1s	-4.71 ± 0.03
	O_2	O 1s	-3.46 ± 0.04
$(CH_3CH_2)O$	O_2	O 1s	-5.30 ± 0.1

(continued)

Table V. (continued)

Compound	Reference	Core Level	E_B(Ref) - E_B(compound) (eV)
cyclo C_2H_4O	CF_4	C 1s	-9.0 ± 0.2
cyclo C_2H_4O	O_2	O 1s	-4.52 ± 0.1
CH_3OH	CF_4	C 1s	-9.1 ± 0.2
CH_3OH	O_2	O 1s	-4.27 ± 0.2
HCOOH	CF_4	C 1s	-6.01 ± 0.2
HCOOH	O_2	O 1s	-2.80, -4.42 ± 0.2
CH_4	CF_4	C 1s	-11.0 ± 0.2 (a)
CO_2	CF_4	C 1s	-4.16 ± 0.2
CO_2	O_2	O 1s	-2.03 ± 0.1
CO	CF_4	C 1s	-5.6 ± 0.2 (a)
CO	O_2	O 1s	-0.53 ± 0.2 (a)
NNO	O_2	O 1s	-1.93 ± 0.2
NNO	N_2	N 1s	-1.18, +2.69 ± 0.2
HCN	N_2	N 1s	-3.80 ± 0.2
HCN	CF_4	C 1s	-10.4 ± 0.2 (b)

Note: O 1s Ref. to the O 1s level of O_2 with lower B.E.

[a] T. D. Thomas, J. Chem. Phys. 52, 1373 (1970).

[b] P. Finn and W. L. Jolly, Lawrence Radiation Laboratory Report UCRL-19671.

case, ΔR is almost zero; much of the shift is due to the dipole of the $-CF_3$ group, but some of it is due to the positive charge induced by the fluorine atoms at the oxygen atom. The CNDO/2 net electronic population at the oxygen atom decreased from 6.26 units of electronic charge to 6.23 between CH_3CH_2OH and CF_3CH_2OH, whereas the population at the hydroxyl carbon atom increased from 3.84 to 3.94. The population at the hydroxyl hydrogen atom decreased from 0.86 to 0.84, however, so the "alternating" inductive effect does not hold here completely; if it did, the electronic population at the hydroxyl hydrogen atom should increase between CH_3CH_2OH and CF_3CH_2OH.

Finally, the method of obtaining atomic populations (or charges) from experimental chemical shifts will be discussed. Essentially, the point-charge model of chemical shifts is assumed:

$$\Delta E_B = -\Delta V_a(Z^0);\ \Delta R = 0$$

$$V_a = kq_a + \sum_j q_j/R^0_{aj} \quad .$$

Here, q_a is the atomic charge at atom a, and R^0_{aj} is the equilibrium internuclear distance between nuclei a and j. In the summation, j cannot equal a. In this model, each chemical shift determines a linear equation for the q's; these equations can be solved simultaneously for the atomic charges if enough chemical shifts are measured, and if enough reference potentials are known. The reference potentials may be obtained from molecular orbital calculations or from electronegativity arguments. The method is noteworthy in that it depends only on internuclear distances

and reference potentials (the k's can be obtained from atomic wavefunctions). Therefore, the method can be applied to any element which possesses a core level. This method has so far been applied to aromatic fluorocarbons[28a,28c] and to symmetrical aliphatic systems.[28b] In most of the applications, good agreement was obtained for the trends in the charges gotten from other methods such as x-ray diffraction data and CNDO/2 or ab initio wavefunctions. However, the method does assume that $\Delta R = 0$; this assumption affects the atomic charges in fluorobenzenes by 0.1 charge unit if ΔR is 1 eV.[28a]

The empirical point-charge model (ACHARGE) was applied here to the fluoromethanes; the results are listed in Table VI. This model clearly gives the β carbon a negative charge in all the fluoroethanes; furthermore, the magnitude of this charge increases with fluorination at the α carbon. Similar results were obtained when this model was applied to the fluorobenzenes.[28a] Thus, the charge distributions obtained by the ACHARGE model for fluorocarbons are very similar to the CNDO/2 charge distributions. This lends further support to the CNDO/2 model, but it should be remembered that the CNDO/2 potential model is very similar to the ACHARGE model, and that to the extent that the CNDO/2 point-charge potential model predicts charges correctly, the CNDO/2 atomic charges will approach those obtained by ACHARGE.

F. Conclusions

CNDO/2 wavefunctions may be used successfully to predict chemical shifts. The CNDO/2 potential models indicate that the relaxation energy

Table VI. ACHARGE Results on Fluorinated Ethanes

Molecule	$q_{\alpha c}$	$q_{\beta c}$	q_H	q_F
CH_3CH_3	0.	0.	0.	--
CH_3CH_2F	+0.233	-0.019	+0.002	-0.226
CH_3CHF_2	+0.493	-0.047	+0.006	-0.234
CH_3CF_3	+0.722	-0.093	+0.025	-0.234

It was assumed that q_c in CH_3CH_3 equalled zero. Chemical shifts were taken relative to CH_3CH_3.

upon core-level ionization must be considered in order to interpret chemical shifts correctly. Relaxation energies show systematic variations with molecular structure; within certain classes of molecules the relaxation energy is constant, allowing the interpretation of chemical shifts in their core-level binding energies in terms of ground state properties alone.

SECTION V. MULTIPLET SPLITTING

A. General

When the inner shells of paramagnetic systems are ionized, multiple peaks may be observed. Much theoretical and experimental work indicates[29] that the multiple peaks are due to the coupling of the unpaired electron in the inner shell with those in the valence shell in the "quasi-bound" final states. This effect was first observed in molecules by the Uppsala group[46] and in transition metals and transition metal compounds by Fadley and Shirley.[30] In the latter cases, the effect can be quite complicated; for example, configuration interaction wavefunctions are required to predict the number of peaks, the peak separation, and the relative intensities in the 3s multiplet splitting in MnF_2.[31] The multiplet splitting observed here is much simpler. The spectra always consist of two peaks, whose relative intensity is always close to the ratio of the multiplicities of the two final states of the ion, and the relative binding energy of the peaks seems to be well-predicted by single-configuration wavefunctions.[32]

The multiplet splitting observed here may be illustrated by the core ionization of the lithium atom. The final states of the ion have the configuration 1s2s; one state is a triplet, and the other is a singlet. The wavefunctions of the ions take the form

$$|1s\uparrow 2s\uparrow| \qquad (^3S)$$

$$\frac{1}{\sqrt{2}}\left(|1s\uparrow 2s\downarrow| - |1s\downarrow 2s\uparrow|\right) \qquad (^1S) \quad .$$

Here it is assumed that each wavefunction consists of a single configuration, and that they are linear combinations of determinants of

one-electron atomic orbitals. If the atomic orbitals are assumed to be the same for both states, the energy of the two states can be represented as $E_0 \pm K$. E_0 is a sum of kinetic energies, nuclear attraction integrals, and coulomb integrals. K is the exchange integral between the inner and outer electrons. In general, if the ground state of the system has a spin S^0, the energy of the high-spin final state is $E_0 - 2SK$ ($S^f = S^0 + 1/2$), and the energy of the low-spin final state is $E_0 + K$ ($S^f = S^0 - 1/2$). This is known as Van Vleck's theorem.[33]

The above theory will here be applied to molecules, as has been done previously,[6] although these workers used initial-state wavefunctions and they assumed that Koopmans' theorem would hold for multiplet splitting. Koopmans' theorem will not be assumed here, and in fact it will be shown that it is a very poor assumption for the interpretation of multiplet splitting in molecules.

B. INDO/2 Predictions

For simplicity, consider a diatomic molecule. Let the molecular orbital containing the unpaired valence electron be the usual linear combination of atomic orbitals centered on atoms a and b:

$$\psi = a\,\phi_a + b\,\phi_b \quad .$$

Assume that center a is the ionized atom. The exchange integral K becomes

$$\int 1s_a(1)\,\psi(1)\,(1/r_{12})\,1s_a(2)\,\psi(2)\,d\tau_1\,d\tau_2 \quad .$$

K breaks up into

$$a^2 \int ls_a \, \phi_a (1/r_{12}) \, ls_a \, \phi_a \, d\tau_1 \, d\tau_2 + 2ab \int ls_a \, \phi_a (1/r_{12}) \, ls_a \, \phi_b \, d\tau_1 \, d\tau_2$$

$$+ b^2 \int ls_a \, \phi_b (1/r_{12}) \, ls_a \, d\tau_1 \, d\tau_2$$

Obviously the first term involves a one-center integral and the second and third terms in K involve two-center integrals. These integrals have been calculated and published[34] for NO by Brion, et al. For the ls orbital on nitrogen, the one-center integral is 0.594 eV ($ls_{1N}2p\sigma_{2N}ls_{3N}2p\sigma_{4N}$ in Brion's notation), the two-center integral in the second term is 0.015 eV ($ls_{1N}2p\pi_{2N}ls_{3N}2p\pi_{40}$); the two-center integral in the third term is so small it is not even listed--it involves the $2p\pi$ orbitals on oxygen, and would be labeled $ls_{1N}2p\pi_{20}ls_{3N}2p\pi_{40}$. A related integral, $ls_{1N}2p\pi_{20}2s_{3N}2p\pi_{40}$, is calculated by Brion to be 0.0043 eV. The largest two-center integral of the exchange type is between the ls orbital and the $2p\sigma$ orbital. For the ls orbital on nitrogen in NO, Brion calculates it to be 0.1929 eV ($ls_{1N}2p\sigma_{20}ls_{3N}2p\sigma_{40}$); the corresponding integral for the 2s orbital on oxygen is 0.070 eV ($ls_{1N}2s_{20}ls_{3N}2s_{40}$). So unless the molecular orbital containing the unpaired electron (s) has a large amount of $2p\sigma$ or 2s character on an atom bonded to the ionized atom, and only a small amplitude to be on the ionized atom, the two-center terms in K are negligible compared to the one-center term. For most molecular systems, however, the unpaired spin is located in π antibonding orbitals.

The molecular orbitals for the various systems studied here were obtained with the INDO/2 method. Rich Martin straightened out the open shell part of this program and calculated the molecular integrals. Since the INDO/2 method does not restrict the spatial orbitals of paired electrons to be identical, the expression for K must be modified somewhat to allow for the small amount of unpaired spin which resides in the molecular orbitals below the highest occupied level. In the unrestricted approach, the one-center term becomes

$$\sum_i [(C_{ia}^{+})^2 - (C_{ia}^{-})^2] K_{ia} \quad . \tag{11}$$

Here, the term in brackets is the net spin density at atom a in molecular orbital i (molecular orbital i is really two orbitals which are almost identical—they are occupied by electrons of paired spin).

Because INDO/2 considers only the valence electrons, some approximation to the final states must be made so that INDO/2 wavefunctions can be used in Eq. (11). The equivalent cores approximation will be used here again. It is assumed that the molecular orbitals of the valence electrons of the two final states will be about the same, and that they will both closely resemble the wavefunction of the valence electrons of the equivalent-cores ion. This approximation neglects in the Hamiltonian the $1/r_{12}$ "exchange" interaction between the unpaired inner electron and the unpaired valence electrons, but for most of the molecules studied here, there is only one unpaired valence electron, so $E_{ion} = E_0 \pm K$, and this neglect will cancel out when taking the difference ΔE_{ion}. That is, K in the

higher (low spin) final state will be slightly smaller than the K calculated with equivalent cores ion wavefunction, and the K in the lower (high spin) final state will be slightly larger than the K calculated with equivalent cores ion wavefunctions.

The calculations presented here neglect electron-electron correlation, of course, because an INDO/2 wavefunction consists of a single configuration. In the case of multiplet splitting, much of the correlation error will cancel out when taking the difference between the energies of the two final states, especially the correlation between the paired electrons--their correlation energies should be almost the same in the two final states. However, one cannot neglect offhand the correlation error between the unpaired electrons in the valence shell and the unpaired electron in the inner shell. It is well-known[35] that the correlation error is greater for the low spin state than for the high spin state. Therefore, neglect of correlation tends to exaggerate the calculated multiplet splitting. In fact, the multiplet splitting calculated for the 3s shell in MnF_2 via single-configuration wavefunctions exceeds the experimental value by 5 eV.[29] Unfortunately, most of the theoretical work on two-electron correlation has been limited to two-electron atoms, so it cannot be applied to molecules.[35] It seems reasonable, however, that the correlation error in multiplet splitting should depend heavily on the number of unpaired valence electrons, and on the overlap between the orbital of the inner electron and those of the unpaired valence electrons--the correlation error would vanish in the limit of zero unpaired valence electrons, or in the limit of an infinite distance

between the inner electron and the unpaired valence electrons. Thus, the correlation error for multiplet splitting in first row molecules should be somewhat smaller than for such splitting in the transition-metal compounds--both the number of unpaired valence electrons and the overlap between inner shells and valence shells are smaller. Perhaps the best indication that correlation errors are small, however, is the almost quantitative agreement between experimental splittings and single-configuration theory obtained for NO by Bagus and Schaefer.[32] The agreement between experiment and theory was within 0.1 eV for both the nitrogen and oxygen splittings. Therefore, it seems that correlation errors can be safely neglected here.

Probably the largest error in the use of INDO/2 wavefunctions is the error in the unpaired electron density at the ionized atom. This error is due partly to the semi-empirical and approximate Hamiltonian of the INDO/2 method and partly to the INDO/2 assumption of orthogonality of atomic orbitals. It is not feasible to estimate the error caused by the INDO/2 Hamiltonian, but the error caused by the assumption of orthogonal atomic orbitals can be analyzed as it was done in the section on chemical shifts.

Consider the case of O_2^+, which is the equivalent-cores ion for the ionization of the nitrogen 1s electron in NO. The unpaired electron occupies an antibonding π orbital, so its "minimum basis" MO must be of the form

$$\psi = a\,\phi_A - a\,\phi_B \quad ,$$

where the atomic orbitals are 2pπ orbitals. Now a must satisfy the normalization requirement that $\int_\tau \psi^* \psi = 1$, or

$$a^2 + a^2 - 2a^2 \int_\tau \phi_a^* \phi_b = 1$$

$$a^2 = 0.5/(1 - \int_\tau \phi_a \phi_b) \quad .$$

Using Slater 2pπ orbitals and the experimental internuclear distance for NO, the denominator becomes 1 - 0.207, and $a^2 = 0.63$. However, the orthogonality assumption of the INDO/2 method requires that $\int_\tau \phi_a \phi_b = 0$, so that $a^2 = 0.5$. Thus the realistic net spin density at atom a exceeds the INDO/2 spin density by about 25%--this amounts to a 0.2 to 0.3 eV difference in the multiplet splitting, and it accounts for much of the difference between the INDO/2 results and the experimental splitting. For atoms bonded to more than one center, this effect will also be sizeble, even for small spin densities on the ionized atom.

C. Trends

The experimental and theoretical values are listed in Table VII. In general, INDO/2 underestimates the experimental values--most of this error is due to the errors in the INDO/2 spin densities. However, the trends among the experimental splittings are fairly well reproduced by the INDO/2 method. In particular, the decrease in N 1s splitting in going from NF_2 to NO_2 is reproduced, as well as the decrease in going from NO to the two nitroxides $(CF_3)_2NO$ and $((CH_3)_3C)_2NO$. Thus the INDO/2 method seems to give a fair account of trends in the uppermost π MO's in these systems.

Table VII. Multiplet Splitting

	Experiment (eV)		Theory (INDO/2) (eV)
NO	Δ_N	1.41(6)	0.96
	Δ_O	0.53(8)	0.35
NO_2	Δ_N	0.68(10)	0.64
	Δ_O	0.65(10)	0.32
NF_2	Δ_N	1.94(7)	1.85
	Δ_F	---	
O_2	Δ_O	1.11(5)	1.05
$(CF_3)_2NO$	Δ_N	0.40(10)	0.15
	Δ_O	0.75(10)	0.31
$((CH_3)_3C)_2NO$	Δ_N	0.54(10)	0.20
	Δ_O	0.45(10)	0.17

Experimental errors are indicated in parentheses; the number in parentheses is the error in the last significant figure.

This is also known from other experimental methods such as ESR[24] and UV photoelectron spectroscopy.[36]

An interesting feature of the INDO/2 calculations is the decrease in the spin density on an atom when its nuclear charge is increased by one, corresponding to inner shell ionization. This generally occurs in spite of the fact that the net electronic population on the atom always increases by 0.5 to 1 electron. Upon examination of a number of CNDO and INDO wavefunctions for both open and closed shell molecules, it became apparent that this effect is not related to the fact that the electron is unpaired, but to its occupation of an anti-bonding orbital. Usually what happens upon core ionization is that the bonding orbitals increase in density at the ionized atom, whereas the anti-bonding orbitals tend to decrease in density. An explanation for this effect was obtained via simple Hückel theory. A bonding and anti-bonding orbital on a diatomic molecule were constructed out of two atomic orbitals, one centered on each atom:

$$\psi_{bond} = a\phi_A + b\phi_B$$

$$\psi_{anti} = b\phi_A - a\phi_B \quad .$$

The coefficients a and b were obtained as usual, but they were expressed as functions of the matrix elements of the Hückel Hamiltonian:[37]

$$a/b = \frac{H_{AA} - \varepsilon_{anti}}{H_{AB}} \quad , \quad a^2 + b^2 = 1$$

$$\varepsilon_{anti} = \frac{H_{AA} + H_{BB}}{2} - \sqrt{\left(\frac{H_{AA} - H_{BB}}{2}\right)^2 + H_{AB}^2} \quad .$$

Here, ε_i is the eigenvalue of the Hückel Hamiltonian for ψ_i;

$$H_{ii} = \int_T \phi_i \mathcal{H}_i \phi_i$$

$$H_{ij} = \int_T \phi_i \mathcal{H}_{ij} \phi_j \quad .$$

H_{ii} represents the kinetic and Coulomb potential energy of an electron at center i, and H_{ij} represents the interaction between nuclei i and j and an electron between them. It was assumed here that

$$H_{ij} = 0.1 \, (H_{ii} + H_{ij}) \quad ,$$

which is close to what is usually done in this field.[37] Figure 13 shows a^2 and b^2 plotted as functions of H_{BB}/H_{AA}. It is clear that the Hückel theory reproduces the trends observed in the INDO/2 wavefunctions--as H_{BB}/H_{AA} is increased, corresponding to ionization of a core electron from atom b, and anti-bonding density on atom b decreases. For first-row elements, core ionization corresponds to an increase in H_{BB}/H_{AA} of 0.2 to 0.25, and a decrease in a^2 of 0.1 to 0.3, which is comparable to the results obtained with INDO/2 wavefunctions.

Thus, Hückel theory indicates that the decrease in spin density upon ionization is directly related to the anti-bonding character of the singly-occupied orbital. Furthermore, both the Hückel and INDO/2 methods indicate that Koopmans' Theorem is inapplicable to multiplet splitting in molecules. Table VIII lists INDO/2 unpaired electron densities for both ground state and ion. It is evident that this density can change considerably upon ionization.

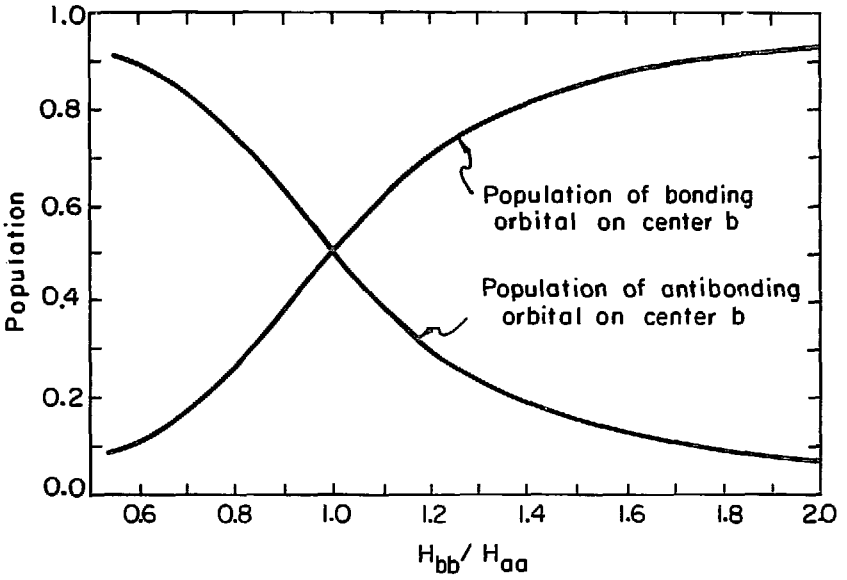

XBL735-2830

Fig. 13. Fractional population in corresponding bonding and antibonding molecular orbitals is plotted versus the ratio of atomic matrix elements. This utilizes the Hückel model; it illustrates the effect of core ionization (increases in H_{22}) at atom b in a diatomic molecule upon fractional atomic populations at atom b.

Table VIII

Molecule	Unpaired Valence Population on Atom i		Unpaired Valence Population on Atom i in Equivalent Cores Ion	
	N	O	$N^{\#}$	$O^{\#}$
NO	0.64	0.36	0.5	0.18 (INDO/2)
O_2	--	1.0	--	1.1 (INDO/2)
	--	1.0	--	0.26 (Ref. 45)
NO_2	0.36	0.32	0.0	0.21 (INDO/2)
NF_2	0.63	--	0.35	-- (INDO/2)
$(CF_3)_2NO$	0.54	0.38	0.25	0.09 (CNDO/2)
$((CH_3)_3C)_2NO$	0.52	0.31	0.19	0.05 (CNDO/2)

D. Data Analysis

Finally, the procedure for obtaining the experimental splittings will be discussed. The spectra were least-squares fitted as usual; the weighted variance turned out to be between 2 and 10, as usual. Some of the splittings were large enough to obtain the intensity ratio of the two peaks from the data--this was always close to the multiplicity ratio of the ions (e.g. a three-to-one ratio for triplet and singlet final states), but always exceeded it by about 15%. This intensity ratio was then assumed to be the same for all the peaks in molecules with the same number of unpaired valence electrons. This constraint aided the fitting of spectra with unresolved peaks. However, the actual values of the splittings were relatively insensitive to the exact value of the ratio. The splittings were also insensitive to whether or not the exciting radiation was assumed to be a spin-orbit doublet, although the weighted variance improved somewhat when the radiation was assumed to be a doublet.

E. Conclusions

The multiplet splittings observed here are predicted fairly well using Van Vleck's Theorem and INDO/2 wavefunctions. The theoretical splittings are generally smaller than experiment, however; this is partly due to the unrealistic "neglect of differential overlap" in the INDO method. The theory indicates that upon core ionization, the migration of unpaired spin in valence levels is considerable. Therefore, Koopmans' Theorem cannot be applied to these multiplet splittings. The theory indicates further that the density of unpaired spin at the atom to be ionized usually decreases upon ionization. This behavior seems to be due to the occupation of antibonding orbitals by the unpaired electrons.

ACKNOWLEDGMENTS

I would like to thank Dr. David A. Shirley for the education and challenge he has provided these past years. He has made many contributions to this thesis, both experimental and theoretical; in particular, he developed the approach to chemical shifts which takes relaxation into account; he also suggested the use of semi-empirical wavefunctions to interpret chemical shifts.

I would also like to thank Charlie Butler for his advice and skill concerning the Berkeley iron-free spectrometer. He was especially helpful with the design and construction of vacuum systems.

I have learned a lot from my colleagues, both past and present, in the Berkeley XPS group. In particular, I would like to acknowledge Salim Banna, Ron Cavell, Norm Edelstein, Chuck Fadley, Pat Finn, Bob Hayes, Bud Kramer, Rich Martin, Bernice Mills, Win Perry, Sefik Suzer, Darrah Thomas, and Jim Wurzbach. Also appreciated is the alternative point of view provided by the solid-state members of the group, Lothar Ley, Steve Kowalczyk, Read McFeely, and Roger Pollak.

I would also like to thank Mrs. Kathy McCracken for lots of good fun, advice, and typing.

The financial support of the Atomic Energy Commission is acknowledged.

REFERENCES

1. Alpha-, Beta-, and Gamma-Ray Spectroscopy, ed. by K. Siegbahn (North-Holland Publishing Co., Amsterdam, 1965).
2. C. S. Fadley, G. L. Geoffroy, S. B. M. Hagström, and J. M. Hollander, Nucl. Instr. Methods 68, 177 (1969).
3. D. S. Evans, Rev. Sci. Instr. 36, 375 (1965).
4. C. S. Fadley, "Core and Valence Electronic States Studied with X-Ray Photoelectron Spectroscopy" (Ph.D. Thesis), Lawrence Radiation Laboratory Report UCRL-19535 (1970).
5. A. B. Cornford, D. C. Frost, F. G. Herring, and C. A. McDowell, J. Chem. Phys. 54, 1872 (1971).
6. K. Siegbahn, C. Nordling, G. Johansson, J. Hedman, P. F. Hédén, K. Hamrin, U. Gelius, T. Bergmark, L. O. Werme, R. Manne, and Y. Baer, ESCA Applied to Free Molecules (North-Holland, 1969).
7. T. D. Thomas, J. Am. Chem. Soc. 92, 4184 (1970).
8. Bernice Mills and Winfield Perry, private communication.
9. Claudette Lederer is a programmer at the Lawrence Berkeley Laboratory.
10. a) E. J. McGuire, Phys. Rev. 185, 1 (1969); b) D. L. Walters and C. D. Bhalla, Phys. Rev. A 3, 1919 (1970).
11. A. Yariv, Quantum Electronics (John Wiley and Sons, 1970).
12. M. K. Born and K. Huang, Dynamical Theory of Crystal Lattices (Oxford University Press, New York, 1954).
13. D. W. Turner, C. Baker, A. D. Baker, and C. R. Brundle, Molecular Photoelectron Spectroscopy (Wiley-Interscience, 1970).
14. G. Herzberg, Molecular Spectra and Molecular Structure, Vol. I., "Spectra of Diatomic Molecules" (Van Nostrand, 1950), pp. 388-394.

15. R. W. Shaw and T. D. Thomas, Phys. Rev. Letters 29, 689 (1972).

16. R. M. Friedman, J. Hudis, and M. L. Pulman, Phys. Rev. Letters 29, 692 (1972).

17. a) W. L. Jolly and D. N. Hendrickson, J. Am. Chem. Soc. 92, 1863 (1970); b) P. Finn, R. K. Pearson, J. M. Hollander, and W. L. Jolly, Inorg. Chem. 10, 378 (1971).

18. D. A. Shirley, Chem. Phys. Letters 15, 325 (1972).

19. H. Hellmann, Einfuhrung in die Quantenchemie (Franz Deuticke, Leipzig and Vienna, 1939), p. 285; R. P. Feynman, Phys. Rev. 56, 340 (1939).

20. S. T. Epstein, A. C. Hurley, R. E. Wyatt, and R. G. Parr, J. Chem. Phys. 47, 1275 (1967).

21. a) M. E. Schwartz, Chem. Phys. Letters 6, 631 (1970); b) H. Basch, Chem. Phys. Letters 5, 337 (1970); c) T. K. Ha and C. T. O'Konski, Chem. Phys. Letters 3, 603 (1969).

22. L. Hedin and A. Johansson, J. Phys. B 2, 1336 (1969).

23. a) C. C. J. Roothaan, J. Chem. Phys. 19, 1445 (1951); b) K. Ruedenberg, C. C. J. Roothaan, and W. Jaunzemis, J. Chem. Phys. 24, 201 (1956).

24. J. A. Pople and D. L. Beveridge, Approximate Molecular Orbital Theories (McGraw-Hill, New York, 1970).

25. a) D. W. Davis and D. A. Shirley, J. Chem. Phys. 56, 671 (1972); b) D. W. Davis, J. M. Hollander, D. A. Shirley, and T. D. Thomas, J. Chem. Phys. 52, 3295 (1970).

26. D. W. Davis and D. A. Shirley, Chem. Phys. Letters 15, 185 (1972).

27. D. A. Shirley, Chem. Phys. Letters 16, 220 (1972).

28. a) D. W. Davis, D. A. Shirley, and T. Darrah Thomas, J. Am. Chem. Soc. 94, 6565 (1972); b) G. D. Stucky, D. A. Matthews, J. Hedman, M. Klasson, and C. Nordling, J. Am. Chem. Soc. 94, 8009 (1972); c) D. T. Clark, D. B. Adams, and D. Kilcast, Chem. Phys. Letters 13, 439 (1972).

29. C. S. Fadley, D. A. Shirley, A. J. Freeman, P. S. Bagus, and J. V. Mallow, Phys. Rev. Letters 23, 1397 (1970).

30. C. S. Fadley and D. A. Shirley, Phys. Rev. A 2, 1109 (1970).

31. S. P. Kowalczyk, L. Ley, R. A. Pollak, F. R. McFeely, and D. A. Shirley, Lawrence Berkeley Laboratory Report LBL-1275.

32. P. S. Bagus and H. F. Schaefer III, J. Chem. Phys. 55, 1474 (1971).

33. J. H. Van Vleck, Phys. Rev. 45, 405 (1934).

34. H. Brion, C. Moser, and M. Yamazaki, J. Chem. Phys. 30, 673 (1959).

35. F. L. Pilar, Elementary Quantum Chemistry (McGraw-Hill, 1968), pp. 377-379.

36. N. Bodor, M. J. S. Dewar, and S. D. Worley, J. Am. Chem. Soc. 92, 19 (1970).

37. C. A. Coulson and A. Streitweiser, Jr., Dictionary of π-Electron Calculations (W. H. Freeman, 1965).

38. C. Manneback, Physica 17, 1001 (1951).

39. a) For N_2, CO, and NO, Ref. 14; b) For NO^+, F. R. Gilmore, J. Quant. Spect. Rad. Transfer 5, 369 (1965), and Ref. 13; c) For HF and NeH^+, V. Bondybey, P. K. Pearson, and H. F. Schaefer III, J. Chem. Phys. 57, 1123 (1972); d) For CF^+, P. A. G. O'Hare and A. C. Wahl, J. Chem. Phys. 55, 666 (1971).

40. Handbook of Chemistry and Physics, ed. by Robert E. Weast (Chemical Rubber Co., 1965).

42. Sefik Suzer measured the CF_3Cl spectrum.

43. W. Heitler, The Quantum Theory of Radiation (Clarendon Press, 1966), p. 185.

44. J. C. Slater, The Quantum Theory of Atomic Structure (McGraw-Hill, 1935), Vols. I and II.

45. P. S. Bagus and H. F. Schaefer III, Lawrence Berkeley Laboratory Nuclear Chemistry Division Annual Report LBL-666 (1971), p. 281.

46. J. Hedman, P. F. Heden, C. Nordling, and K. Siegbahn, Phys. Letters 29A, 178 (1969).

47. NBS Technical Note 438, compiled by Morris Krauss (1967).

48. For the experimental geometry of NOF, see Ref. 40. For the calculated geometry of NF_2^+, see Ref. 47.

49. T. Koopmans, Physica 1, 104 (1933).

50. H. Basch and L. C. Snyder, Chem. Phys. Letters 3, 333 (1969).